International Journal of
Molecular Sciences

MDPI

Article

A Mouse Systems Genetics Approach Reveals Common and Uncommon Genetic Modifiers of Hepatic Lysosomal Enzyme Activities and Glycosphingolipids

Anyelo Durán [1], David A. Priestman [2], Macarena Las Heras [1], Boris Rebolledo-Jaramillo [1], Valeria Olguín [1], Juan F. Calderón [1,3], Silvana Zanlungo [4], Jaime Gutiérrez [5], Frances M. Platt [2] and Andrés D. Klein [1,*]

1 Centro de Genética y Genómica, Facultad de Medicina, Clínica Alemana Universidad del Desarrollo, Santiago 7610658, Chile
2 Department of Pharmacology, University of Oxford, Oxford OX1 3QT, UK
3 Research Center for the Development of Novel Therapeutic Alternatives for Alcohol Use Disorders, Santiago 7610658, Chile
4 Department of Gastroenterology, Faculty of Medicine, Pontificia Universidad Católica de Chile, Santiago 8330033, Chile
5 Cellular Signaling and Differentiation Laboratory, School of Medical Technology, Health Sciences Faculty, Universidad San Sebastian, Santiago 7510602, Chile
* Correspondence: andresklein@udd.cl

Abstract: Identification of genetic modulators of lysosomal enzyme activities and glycosphingolipids (GSLs) may facilitate the development of therapeutics for diseases in which they participate, including Lysosomal Storage Disorders (LSDs). To this end, we used a systems genetics approach: we measured 11 hepatic lysosomal enzymes and many of their natural substrates (GSLs), followed by modifier gene mapping by GWAS and transcriptomics associations in a panel of inbred strains. Unexpectedly, most GSLs showed no association between their levels and the enzyme activity that catabolizes them. Genomic mapping identified 30 shared predicted modifier genes between the enzymes and GSLs, which are clustered in three pathways and are associated with other diseases. Surprisingly, they are regulated by ten common transcription factors, and their majority by miRNA-340p. In conclusion, we have identified novel regulators of GSL metabolism, which may serve as therapeutic targets for LSDs and may suggest the involvement of GSL metabolism in other pathologies.

Keywords: metabolism; lysosomal enzymes; glycosphingolipids; systems genetics; modifier genes

Citation: Durán, A.; Priestman, D.A.; Las Heras, M.; Rebolledo-Jaramillo, B.; Olguín, V.; Calderón, J.F.; Zanlungo, S.; Gutiérrez, J.; Platt, F.M.; Klein, A.D. A Mouse Systems Genetics Approach Reveals Common and Uncommon Genetic Modifiers of Hepatic Lysosomal Enzyme Activities and Glycosphingolipids. *Int. J. Mol. Sci.* **2023**, *24*, 4915. https://doi.org/10.3390/ijms24054915

Academic Editor: Paola Pontrelli

Received: 7 January 2023
Revised: 7 February 2023
Accepted: 15 February 2023
Published: 3 March 2023

1. Introduction

Hydrolytic enzymes are abundant in lysosomes [1]. In a healthy cell, the biosynthesis and catabolism of macromolecules are subject to regulatory mechanisms that maintain cellular homeostasis [2]. The degradative processes in lysosomes are controlled by their own enzymes [3,4]. Lysosomes play a central role in several biological processes, including energy metabolism, signaling, plasma membrane repair, secretion, and others [3]. Loss-of-function variants in genes encoding lysosomal proteins cause lysosomal storage disorders (LSDs), a group of diseases characterized by intracellular buildup of partially degraded material [5]. Growing evidence suggests that variants in lysosomal genes increase the risk of developing Parkinson's disease (PD) [6,7].

In the sphingolipidoses, a subset of LSDs, glycosphingolipids (GSLs) accumulate in late endocytic organelles (late endosomes/lysosomes) and participate in their pathological cascades [8]. Current treatments for LSDs include substrate reduction therapy (SRT), which aims to reduce the rate of biosynthesis of stored substrates [5,9,10], and enzyme replacement therapies (ERT) aimed at replacing a deficient enzyme [11,12]. Emerging treatments include gene and cell therapies [13–15] and chaperones for improving enzyme folding and trafficking [16]. Although there is a range of therapeutic options for LSDs,

they have limitations, such as tissue accessibility [17], antibody-mediated reaction [18], cost [19], and others. So far, therapies aimed at increasing enzyme activity or reducing lipid levels by modulating a second (modifier) gene have not been studied. In this context, a deeper understanding of the regulatory mechanisms that govern GSLs metabolism must be uncovered to fully develop this approximation.

Genome-wide association studies (GWAS) in humans and systems genetics strategies, which include gene mapping in model organisms, have identified genetic regulators of physiological and pathophysiological processes [20–22]. The Hybrid Mouse Diversity Panel (HMDP) has been a useful tool because genomes and tissue transcriptomes are freely available, allowing the combination of modifier gene mapping by GWAS and pathway analysis [23,24]. In this study, we have analyzed the activities of 11 lysosomal enzymes and several of their natural substrates in 25 strains of the HMDP panel followed by gene mapping and transcript integration. We identified a lack of correlation between most enzyme activities and their mRNA levels. Similarly, most substrates had no association between their levels and the enzyme activity that catabolizes them. Finally, we mapped putative modifier genes of each lysosomal enzyme and GSL by GWAS. We found associations between the mRNA levels of many modifier genes and enzyme activities or GSL levels. We clustered the putative modifiers in pathways and identified common and uncommon genetic regulators between GSLs and lysosomal enzymes, including transcription factors that regulate them. Our discoveries may help develop novel therapeutics for diseases with altered lysosomal enzyme activities and GSLs.

2. Results

2.1. High Variability in the Hepatic Activity of Lysosomal Enzymes across Mouse Strains

We measured hepatic enzyme activity of β-hexosaminidase A and B (defective in Tay-Sachs and Sandhoff disease, respectively), α-neuraminidase (defective in Sialidosis/Mucolipidosis Type I), α-galactosidase A and B (defective in Fabry and Schindler disease), β-D-galactosidase (defective in GM1 Gangliosidosis), α-glucosidase (defective in Pompe), chitotriosidase (elevated in Gaucher disease), α-L-fucosidase (defective in fucosidosis), lysosomal acid phosphatase (elevated in patients with Gaucher), and Tartrate-resistant acid phosphatase (TRAP; altered in Gaucher disease) by fluorimetry in liver samples derived from 25 inbred mice strains using 4-methylumbelliferone (4-MU) based artificial substrates. We observed significant variability in the average enzymatic activity between the different strains (ANOVA $p \leq 0.05$) (Figure 1). We did not find changes in α-galactosidase A, lysosomal acid phosphatase, and TRAP activities across the tissues analyzed (Figure 1d,j,k). We observed unique activity distribution patterns across the strains for the other enzymes, suggesting specific modifiers for each enzyme.

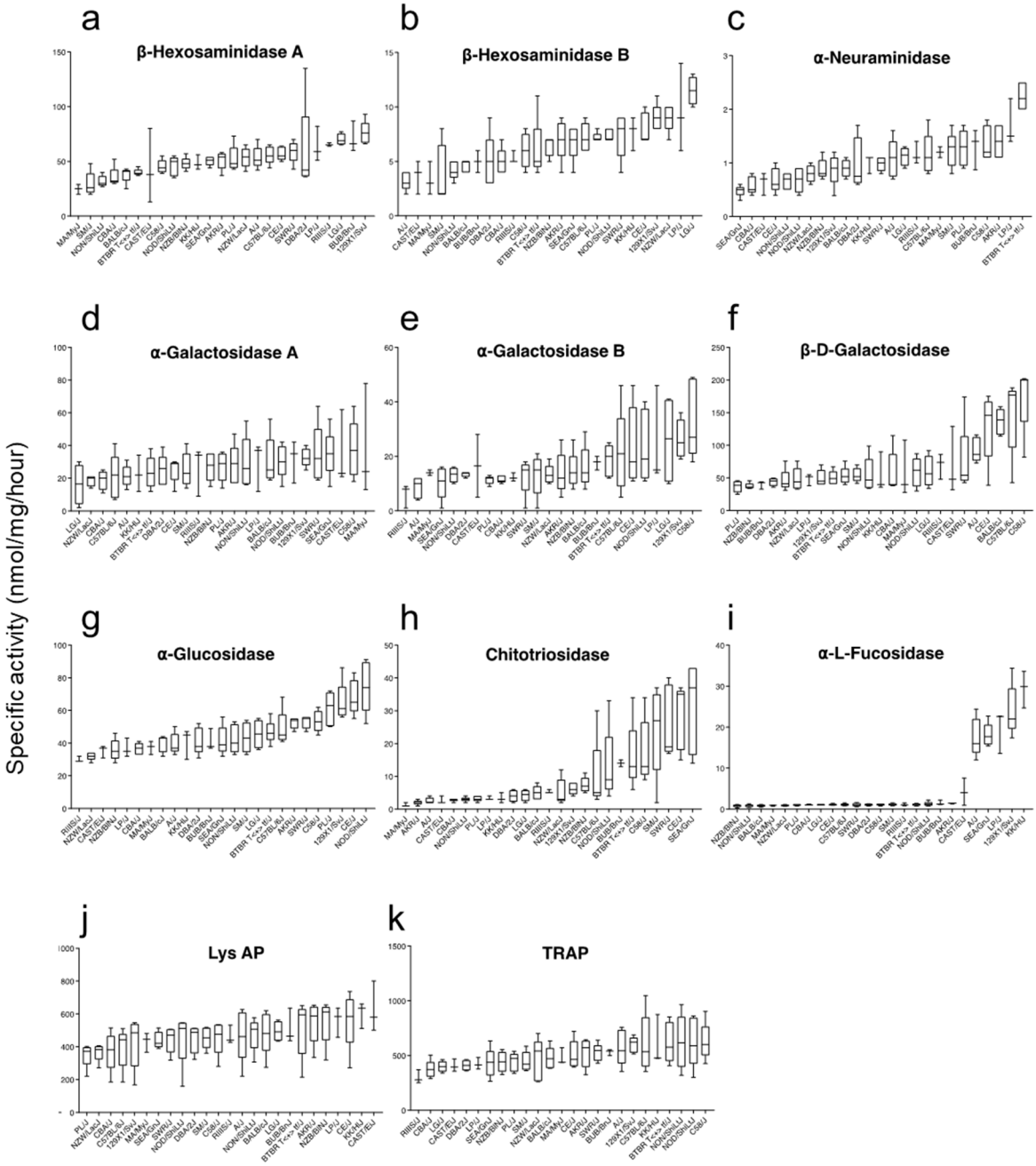

Figure 1. Hepatic variation in lysosomal enzyme activities across inbred strains. Enzyme activity are expressed as nmol/mg/hour. (**a**) Distribution of β-Hexosaminidase A. (**b**) β-Hexosaminidase B. (**c**) α-Neuraminidase. (**d**) α-galactosidase A. (**e**) α-galactosidase B. (**f**) β-D-galactosidase. (**g**) α-Glucosidase. (**h**) Chitotriosidase. (**i**) α-L-Fucosidase. (**j**) Lysosomal acid phosphatase. (**k**) Tartrate-resistant acid phosphatase, activity in the liver of 25 mouse inbred strains. Values are presented as median (n = 3–5 per strain).

2.2. Lack of Correlation between the Enzyme Activity and Its mRNA Levels

Advantages of using tissues derived from the HMDP panel of inbred mouse strains include the fact that their genomes are sequenced, and transcriptomic data are available. Thus, we analyzed potential correlations between the genes encoding lysosomal enzymes and their activities. Recently we described the natural variation of hepatic acid β-glucocerebrosidase levels across many different mouse strains and included them in this analysis [20]. We did not identify significant correlations between enzyme activity and

its transcript levels (Figure 2), with the only exception being *Glb1*, the gene encoding for β-D-galactosidase (r = 0.5775; $p \leq 0.002$) (Figure 2c). These results indicate that mRNA levels are a poor proxy for enzyme activities.

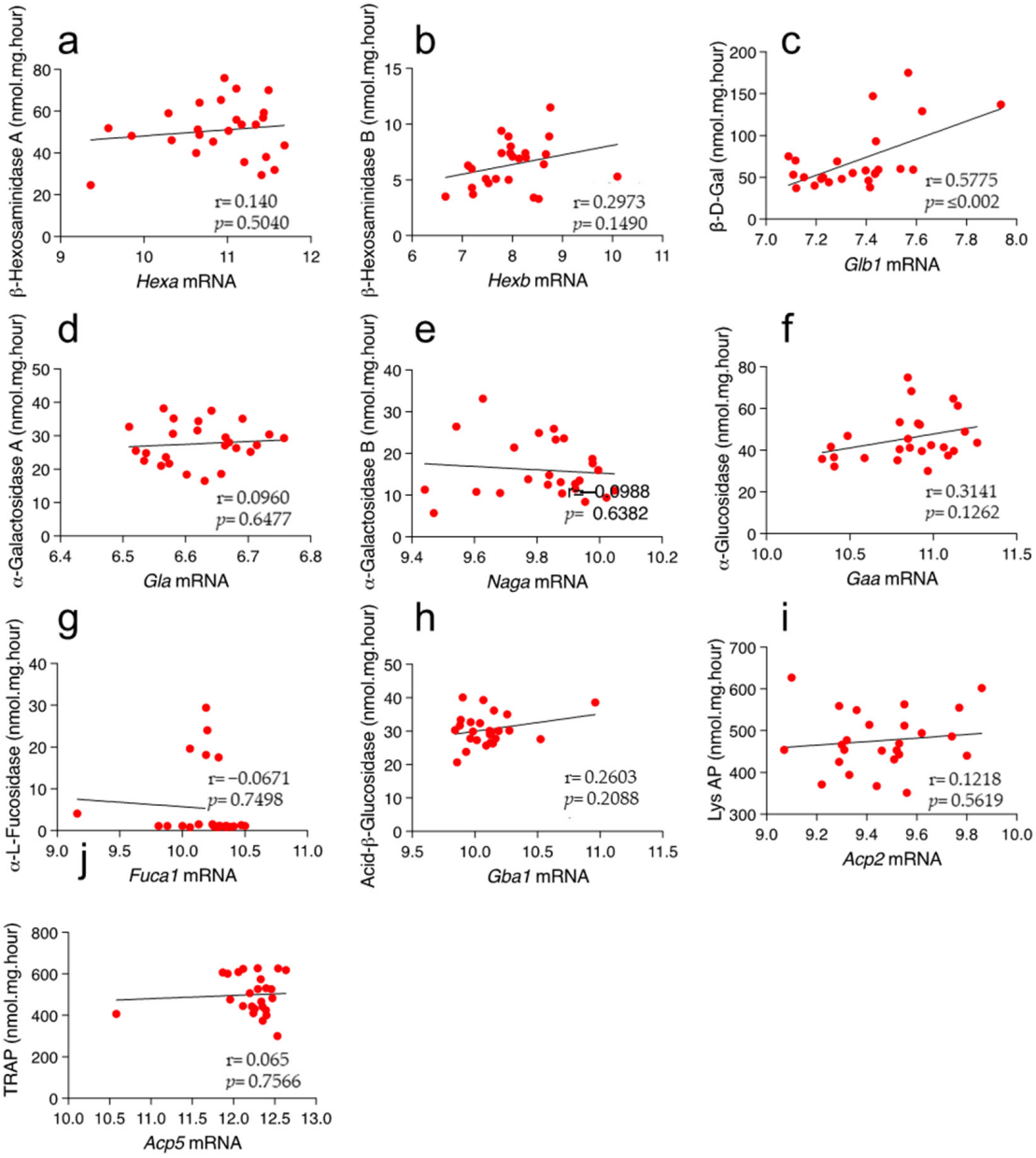

Figure 2. Correlation between expression levels and enzymatic activity in liver of mouse inbred strains. Each dot represents a mouse strain. (**a**) β-Hexosaminidase A. (**b**) β-Hexosaminidase B. (**c**) β-D-galactosidase. (**d**) α-galactosidase A. (**e**) α-galactosidase B. (**f**) α-Glucosidase. (**g**) α-L-Fucosidase. (**h**) Acid-β-glucosidase. (**i**) Lysosomal acid phosphatase. (**j**) Tartrate-resistant acid phosphatase. The Pearson's correlation was performed using 23 strains of mice. Enzyme activities are expressed as nmol/mg/hour and mRNA levels, which were downloaded from repository GSE16780 UCLA Hybrid MDP Liver Affy HT M430A [24] are expressed as log2 transformed. r, correlation; *p*, *p*-value.

2.3. High Variability in the Hepatic Glycosphingolipid Levels across Mouse Strains

Next, we measured the levels of GSLs in livers of the inbred mice strains in which we had access to enough material for three biological replicates (23/25) by Normal Phase-High-Performance Liquid Chromatography (NP-HPLC). We observed significant variability in GSLs among the strains, especially in total GSLs, GM3-Gc, GM2-Gc, GM1agc, GM3,

Gb3, GM1a, GM1b, GD1b, and GD1a (Figure 3). For example, the levels of GM3-Gc were significantly increased (ANOVA $p < 0.0001$) in NOD/ShiLtJ compared with the other samples (Figure 3b). These results indicate that GSLs levels vary across strains.

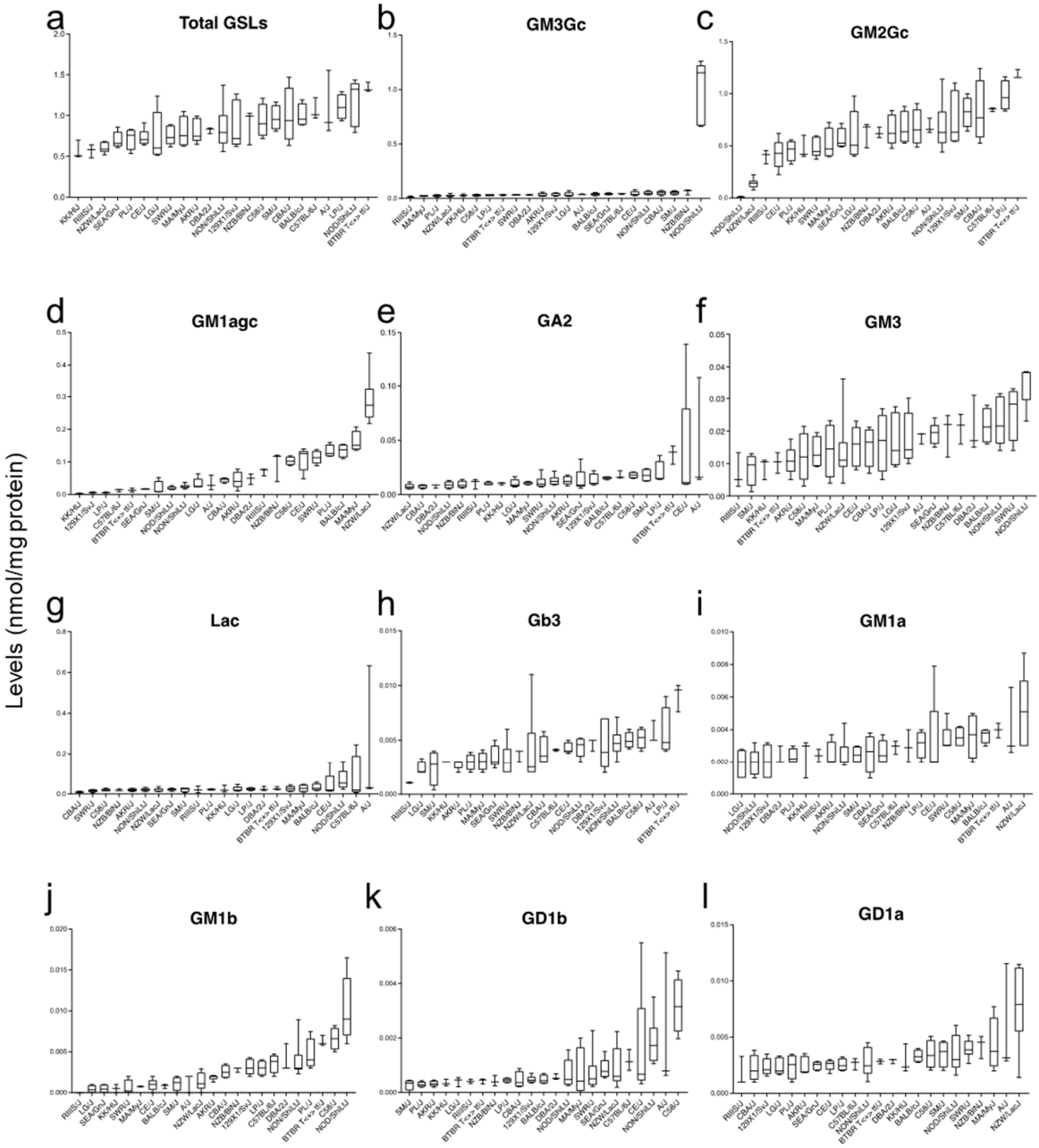

Figure 3. Variation of glycosphingolipids (GSLs) levels in liver of mouse inbred strains. Distribution of glycosphingolipids levels expressed as nmol/mg protein; (**a**) total GSLs (GM3-Gc + GM2-Gc + GM1agc + GA2 + GM3 + LacCer + Gb3 + GM1a + GM1b + GD1b + GD1a) levels. (**b**) GM3-Gc. (**c**) GM2-Gc. (**d**) GM1agc. (**e**) GA2. (**f**) GM3. (**g**) LacCer (Lac). (**h**) Gb3. (**i**) GM1a. (**j**) GM1b. (**k**) GD1b. (**l**) GD1a, in the liver of 23 mouse inbred strains. Values are presented as median (n = 3–5 per strain).

2.4. Correlations between the GSLs and the mRNA Levels of the Biosynthetic Genes

A possibility is that GSL levels could correlate with their biosynthesis rate. Since we started from frozen tissues, we could not test this directly. Instead, we utilized the transcriptomic data available from the repository GSE16780 UCLA Hybrid MDP Liver Affy HT M430A [24]. We found transcript probes for 21 mRNA of the 21 anabolic en-

zymes of the GSLs pathway and four GSL transfer proteins. The analyzed gene list of the biosynthetic pathway is presented in the Supplementary Table S1. The expression values were organized according to GSLs levels from lowest to highest and presented as a heatmap. The analysis showed significant correlations for Cgt (r = −0.4263; $p = 0.042$) with total GSLs (Figure 4a). For GM2-Gc with Cgt (r = −0.4582; $p = 0.0279$), Galgt1 (r = 0.6078; $p = 0.0021$), A4galt (r = 0.4903; $p = 0.0176$), Gltp (r = −0.454; $p = 0.0296$) (Figure 4b). GM3 levels correlated with Galgt1 (r = −0.579; $p = 0.0038$), Gltp (r = 0.4151; $p = 0.0489$) (Figure 4c). GM1a with Col4a3bp (r = 0.4458 $p = 0.033$) (Figure 4d). GM3-Gc is associated with Galgt1 (r = −0.9591, $p \leq 0.0001$) and it was the most significant correlation (Figure 4e). GM1agc levels with Slc17a2 (r = 0.4163; $p = 0.0482$) (Figure 5f). Gb3 with A4galt (r = 0.6011, $p = 0.0024$) (Figure 4g) and GM1b with Galgt1 (r = −0.5764; $p = 0.004$) and St8sia5 (r = −0.4194, $p = 0.0046$) (Figure 4h). No significant correlations were found between the majority of GSLs and biosynthetic genes (Supplementary Table S2); thus, we analyzed potential correlations between GSL levels and the enzyme activity that catabolizes them across the mouse panel.

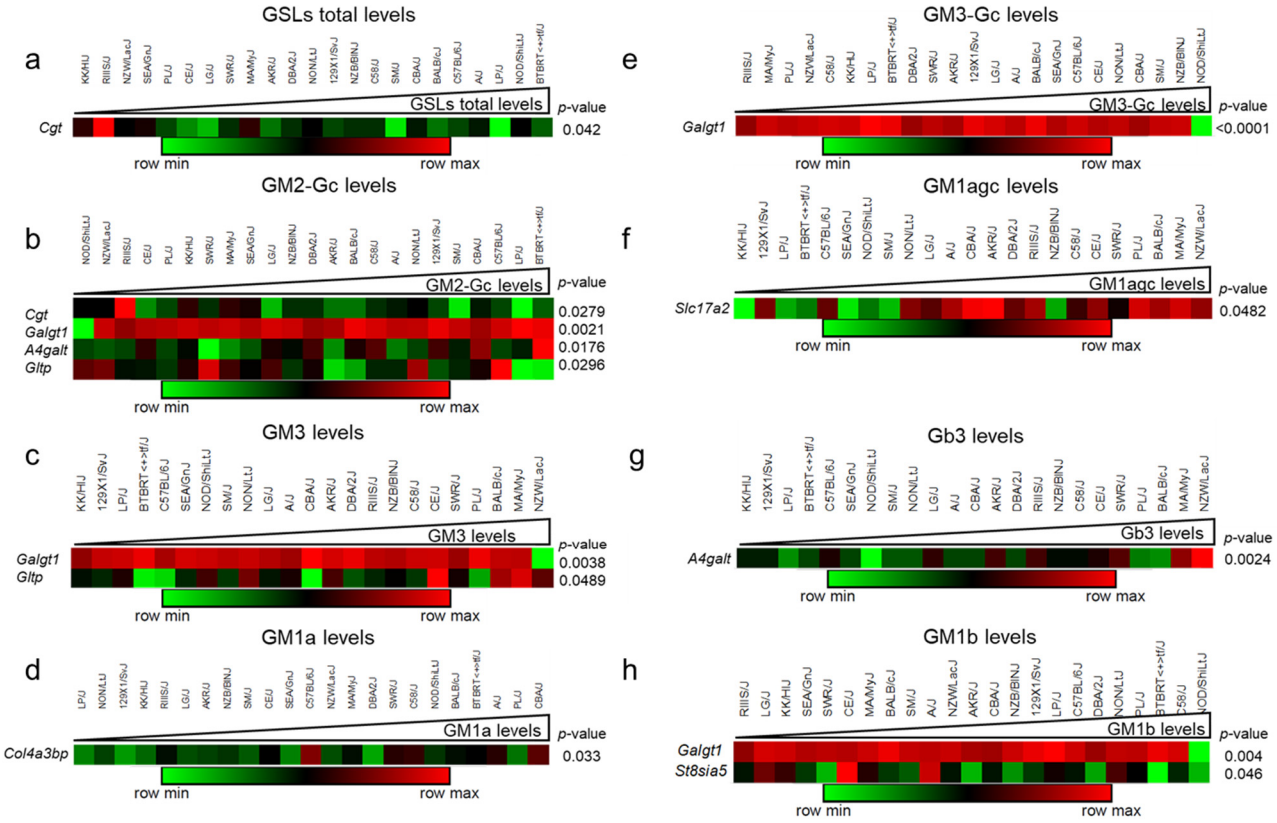

Figure 4. Correlations between GSLs and the mRNA levels of the GSL biosynthetic genes. (**a**) total GSL. (**b**) GM2-Gc. (**c**) GM3. (**d**) GM1a. (**e**) GM3-Gc. (**f**) GM1agc. (**g**) Gb3. (**h**) GM1b levels. Only the genes with significant p values with its trait using Pearson's correlations ($p \leq 0.05$) were plotted.

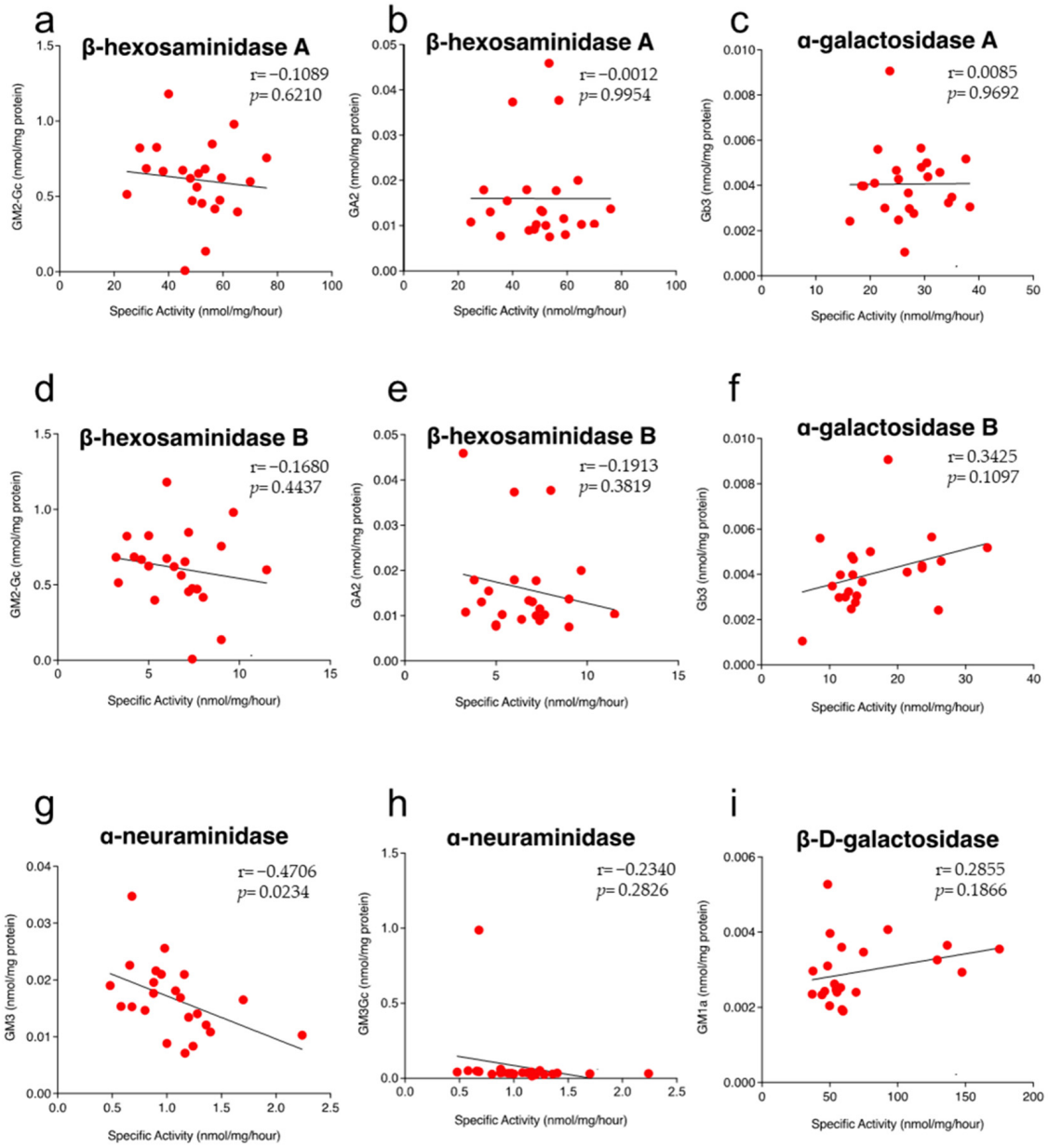

Figure 5. Correlation of hepatic lysosomal enzyme activities and specific substrates levels. Each dot represents a mouse strain. (**a**) HexA vs. GM2-Gc. (**b**) HexA vs. GA2. (**c**) α-Gal A vs. Gb3. (**d**) HexB vs. GM2-Gc. (**e**) HexB vs. GA2. (**f**) α-Gal B vs. Gb3. (**g**) Neu vs. GM3. (**h**) Neu vs. GM3-Gc. (**i**) β-D-Gal vs. GM1a; r, Pearsons' correlation; *p*, *p*-value.

2.5. Lack of Correlation between Hepatic Lysosomal Enzyme Activity and Their Natural Substrates across Mouse Strains

It is possible to speculate that the strains that present high activity of a particular enzyme should have reduced levels of its natural substrate because the enzyme catabolizes it. Unexpectedly, for most enzymes, we did not find significant correlations between the GSL levels and the enzyme activity that degrades it (Figure 5), except for neuraminidase and GM3-Gc (r = −0.4706; p = 0.0234) (Figure 5g). These results suggest that for most strains, the rate of biosynthesis and/or uptake of GSLs varies along with the catabolic rates which most likely are genetically regulated.

2.6. Identification of Putative Modifier Genes of Lysosomal Enzyme Activity and Sphingolipids Levels

To identify genetic regulators, we conducted genome-wide association studies with a quality control analysis that considered the population structure of the HMDP panel strains to reduce false associations [25,26]. We used enzyme activity levels as a trait and included the β-glucosidase activity, which we reported previously in the same and a few other strains [20]. For all the enzymes together, we identified 211 significant Single Nucleotide Variants (SNVs) that passed the empiric threshold of significance $p \leq 4.1 \times 10^{-6}$ ($-$log10P = 5.39), previously calculated by permutations [21,22,26], while the Bonferroni threshold was $p \leq 3.9 \times 10^{-7}$ [26]. These SNVs were located in different genomic regions (exonic, intronic, UTR3, downstream, and intergenic) (Table 1, Supplementary Table S3) in a total of 137 non-redundant genes. Similarly, we identified 3215 SNVs associated with GSLs levels (1744 non-redundant genes) whose variants are located in different genomic regions (Table 1, Supplementary Table S3). These analyses indicated that our strategy has sufficient power to map putative modifier genes.

Table 1. Summary of the putative modifier genes of enzymatic activity and GSLs levels identified by GWAS.

	Trait	Gene	Region	Chr	Position	Ref	Alt	*p*-Value	SNV $p < 10^{-6}$	Non-Redundant Genes
lysosomal enzymes	α-Galactosidase A	*Stard4*	intergenic	18	33494519	C	T	2.88×10^{-6}	1	1
	α-Galactosidase B	*Barhl2*	intergenic	5	106880801	T	C	4.10×10^{-7}	1	1
	GCase	*Dmrtc2*	UTR3	7	25662483	A	G	7.46×10^{-7}	2	2
		Arhgef1	UTR3	7	25711350	G	T	7.46×10^{-7}		
	α-Glucosidase	*Tiam2*	intergenic	17	3338741	T	C	1.89×10^{-6}	3	2
		Tfb1m	intronic	17	3557483	G	T	1.89×10^{-6}		
	β-D-Galactosidase	*Lyplal1*	intergenic	1	188026657	A	G	9.09×10^{-9}	88	70
		4930433B08Rik	intergenic	3	18512557	A	G	2.32×10^{-8}		
		Peak1	intronic	9	56165236	T	C	2.32×10^{-8}		
		Imp3	intergenic	9	56793621	A	G	2.32×10^{-8}		
		Scamp2	intronic	9	57409841	T	C	2.32×10^{-8}		
		Loxl1	intergenic	9	58188292	A	G	2.32×10^{-8}		
		1700072B07Rik	intergenic	9	58256079	G	A	2.32×10^{-8}		
		Arih1	intergenic	9	59348484	C	T	2.32×10^{-8}		
		Pkm	intronic	9	59506197	A	T	2.32×10^{-8}		
		Iqch	intronic	9	63413504	A	G	2.32×10^{-8}		
	Chitotriosidase 1	*Wdr89*	intergenic	12	76773815	T	C	2.45×10^{-8}	8	3
		Syne2	intronic	12	76961077	T	C	2.45×10^{-8}		
		Chchd6	intergenic	6	89566833	A	G	1.37×10^{-6}		
	α-L-Fucosidase	*Myom3*	intergenic	4	135400588	C	T	6.06×10^{-17}	103	56
		Vps45	intronic	3	95807768	C	T	1.13×10^{-1}		
		Hist2h2be	downstream	3	96027761	G	A	1.13×10^{-1}		
		Tet2	intergenic	3	133254547	A	C	1.13×10^{-1}		
		Zfp46	UTR3	4	135847850	A	G	1.13×10^{-1}		
		Hnrnpr	intergenic	4	135915162	C	T	1.13×10^{-1}		
		E2f2	UTR3	4	135750026	C	T	8.13×10^{-9}		
		Stkld1	intronic	2	26790736	A	C	6.67×10^{-8}		
		Xkr7	intergenic	2	152887679	G	A	6.67×10^{-8}		
		Ttpal	intronic	2	163432431	A	G	6.67×10^{-8}		
	TRAP	*Zfat*	intronic	15	68115989	A	C	7.70×10^{-7}	5	2
		Mir30d	intergenic	15	68244382	C	T	7.72×10^{-7}		

Table 1. *Cont.*

	Trait	Gene	Region	Chr	Position	Ref	Alt	*p*-Value	SNV $p < 10^{-6}$	Non-Redundant Genes
GSLs	GD1a	*Ctnnbl1*	intronic	2	157632357	T	A	1.46×10^{-7}	37	26
		Rap2b	intergenic	3	61765728	A	C	1.46×10^{-7}		
		Arhgef26	intronic	3	62232093	C	T	1.46×10^{-7}		
	GA2	*Dars*	intergenic	1	130350640	C	T	1.09×10^{-11}	190	103
		Abca16	intronic	7	127596308	G	A	1.09×10^{-11}		
		E130201H02Rik	intergenic	7	127763574	G	A	1.09×10^{-11}		
		Vwa3a	intronic	7	127887001	G	A	1.09×10^{-11}		
		Eef2k	intronic	7	127993389	A	G	1.09×10^{-11}		
	LacCer	*Tgs1*	intergenic	4	3571870	C	G	1.38×10^{-12}	1152	723
		Dtnb	intronic	12	3586440	C	T	1.38×10^{-12}		
		Lyn	intronic	4	3673421	A	G	1.38×10^{-12}		
		Ghr	intergenic	15	3696333	T	C	1.38×10^{-12}		
		1810055G02Rik	intergenic	19	3731017	G	A	1.38×10^{-12}		
		Bambi	intergenic	18	3826103	C	A	1.38×10^{-12}		
		Hnf4g	intergenic	3	3989664	G	T	1.38×10^{-12}		
		Dnajc27	UTR3	12	4106955	G	C	1.38×10^{-12}		
		Mterf1b	intergenic	5	4503200	A	G	1.38×10^{-12}		
		Impad1	intergenic	4	4885958	C	G	1.38×10^{-12}		
	GD1b	*Ahctf1*	intergenic	1	181812047	C	A	1.03×10^{-8}	23	17
		Psen2	intronic	1	182170093	C	T	1.03×10^{-8}		
		Fhit	intronic	14	11843484	G	A	1.03×10^{-8}		
	GM3Gc	*Cdk6*	intergenic	5	3011917	T	C	1.51×10^{-31}	1811	995
		Insr	intergenic	8	3058687	C	T	1.51×10^{-31}		
		Eif4enif1	intronic	11	3143753	G	A	1.51×10^{-31}		
		Tiam2	intronic	17	3417745	T	C	1.51×10^{-31}		
		Ppp6r3	intronic	19	3539614	C	T	1.51×10^{-31}		
		Tfb1m	intronic	17	3540913	C	A	1.51×10^{-31}		
		1700102H20Rik	intergenic	17	3611518	G	A	1.51×10^{-31}		
		Pex1	intronic	5	3632859	T	G	1.51×10^{-31}		
		Ankib1	intronic	5	3711311	C	T	1.51×10^{-31}		
		Ankib1	intronic	5	3778272	C	T	1.51×10^{-31}		
	GM1b	*Hrasls*	intergenic	16	29161604	A	C	2.71×10^{-6}	2	1

2.7. Correlations between the Traits and the mRNA Levels of Putative Modifiers

To prioritize the putative modifier genes that could regulate each enzyme, we searched for correlations between the transcript levels of putative modifier genes and their traits (enzyme activity and GSL levels, respectively) (Figure 6). We found transcript probes for 67 mRNA of the 137 putative modifiers of the enzymes. The expression values were organized according to enzyme activity from lowest to highest and presented as a heatmap. The analysis showed significant correlations in Fip1l1 (r = −0.4462; $p = 0.0254$) with α-L-fucosidase (Figure 6a). For β-D-galactosidase with Lyplal1 (r = −0.702; $p = <0.0001$), Arrdc4 (r = 0.627; $p = 0.0008$), Pde2a (r = 0.5306; $p = 0.0064$), Glb1 (r = 0.5753; $p = 0.0026$), Bptf (r = 0.5135; $p = 0.0087$), Oxr1 (r = −0.447; $p = 0.0251$) (Figure 6b). No significant correlations were found for the other enzymes analyzed. We used SIFT to explore the impact of genetic variants on the genes identified by GWAS (benign or deleterious changes) associated with changes in enzyme activity [27], because the full genomes of the strains are known [28]. This strategy identified 308 predicted deleterious variants (Supplementary Table S4) in 43 of the 67 genes whose functions are related to organelle biogenesis (Chchd6) [29], intracellular signaling (Pde4dip) [30], and tissue development (Fam181b) [31], among others. These results suggest that amino acid substitution could affect protein function and signaling pathways leading to changes in enzyme activity.

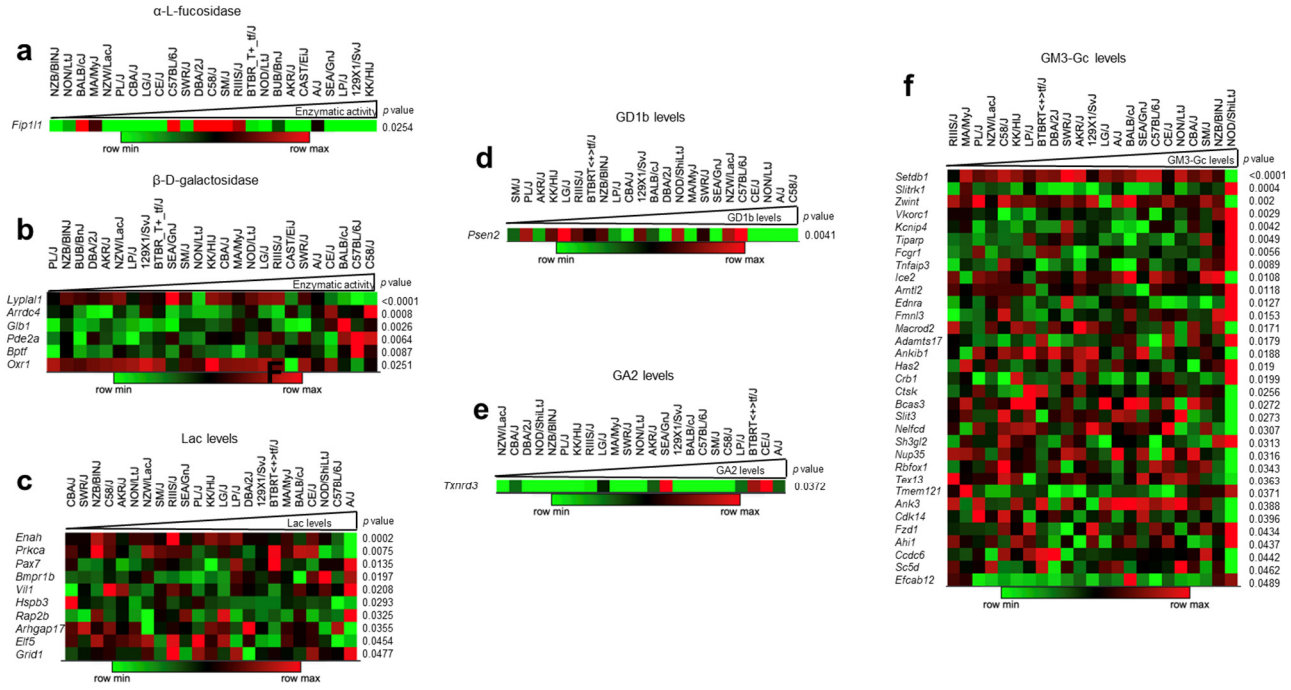

Figure 6. Correlations between the traits (enzyme activities or GSLs) and the mRNA levels of the identified modifier genes. (**a**) α-L-Fucosidase. (**b**) β-D-galactosidase. (**c**) LacCer (Lac). (**d**) GD1b. (**e**) GA2. (**f**) GM3-Gc. Only the genes with significant p values with its trait using Pearson's correlations ($p \leq 0.05$) were plotted.

The same analysis was performed to identify putative modifiers of GSL levels (Figure 6c–f). For 1744 non-redundant SNVs, we found expression values for 994 genes. The analysis identified 45 significant correlations, of which 33 were correlated with GM3-Gc levels, 10 genes with LacCer, and one gene with GD1b and GA2 (Figure 6c–f). Overall, we recorded 4.9% (52/1061) of significant correlations distributed between the two traits. We also explored the impact of genetic variants associated with changes in GSLs with SIFT [27]. This strategy identified 515 deleterious variants predicted to disrupt the protein structure (Supplementary Table S4) in 132 genes related to DNA methyltransferase activity (Setdb1) [32] and synapse (Slitrk1) [33], among others.

2.8. Enrichment Analysis and Common Modifier Genes between Glycosphingolipids Levels and Lysosomal Enzyme Activities

If there is an orchestrated regulation of GSL levels and the enzymes that degrade them, it would be expected to observe enrichment in common pathways [34]. We therefore utilized gProfiler [35] to perform enrichment analysis using the putative modifier genes lists. For the modifier of enzyme activities, we found significantly associated pathways such as cell periphery ($p = 5.9 \times 10^{-4}$), plasma membrane ($p = 2.4 \times 10^{-3}$), and integral components of the plasma membrane ($p = 2.6 \times 10^{-2}$) (Figure 7b), which could be related to endocytic processes necessary to deliver key molecules to the lysosome, including the lysosomal enzymes that can be recycled from the extracellular space. Significant biological processes analysis included regulation of cellular processes ($p = 3.9 \times 10^{-2}$) (Figure 7d) (Supplementary Table S5). We did not find significant enrichment for the molecular function category. For GSLs, we observed enrichment in terms like cytoplasm ($p = 3.5 \times 10^{-28}$), cell junction ($p = 7 \times 10^{-21}$), synapse ($p = 4.6 \times 10^{-19}$), and 70 other pathways related to cellular components (Figure 7a; Supplementary Table S5). Many of these pathways require cellular membranes, where GSLs play a structural role. Significantly enriched Gene Ontology (GO) terms included protein binding ($p = 9.1 \times 10^{-31}$), ion binding ($p = 8.8 \times 10^{-14}$), binding ($p = 2.3 \times 10^{-13}$), ATP binding ($p = 9.4 \times 10^{-13}$), carbohydrate

derivate binding ($p = 1.8 \times 10^{-1}$), and 27 other pathways related to molecular functions (Supplementary Table S5). Biological processes terms revealed 328 pathways, including system development ($p = 4.3 \times 10^{-39}$), anatomical structure development (5.6×10^{-38}), and multicellular organism development ($p = 1.4 \times 10^{-37}$). We searched for the overlap between the cellular component domains of modifiers of enzyme activity and GSLs, which resulted in three common pathways (GO:0071944—cell periphery, GO:0005886—plasma membrane, and GO:0005887—integral component of plasma membrane) (Figure 7c) and one pathway associated with biological processes (GO:0050794; regulation of cellular process) (Supplementary Table S5).

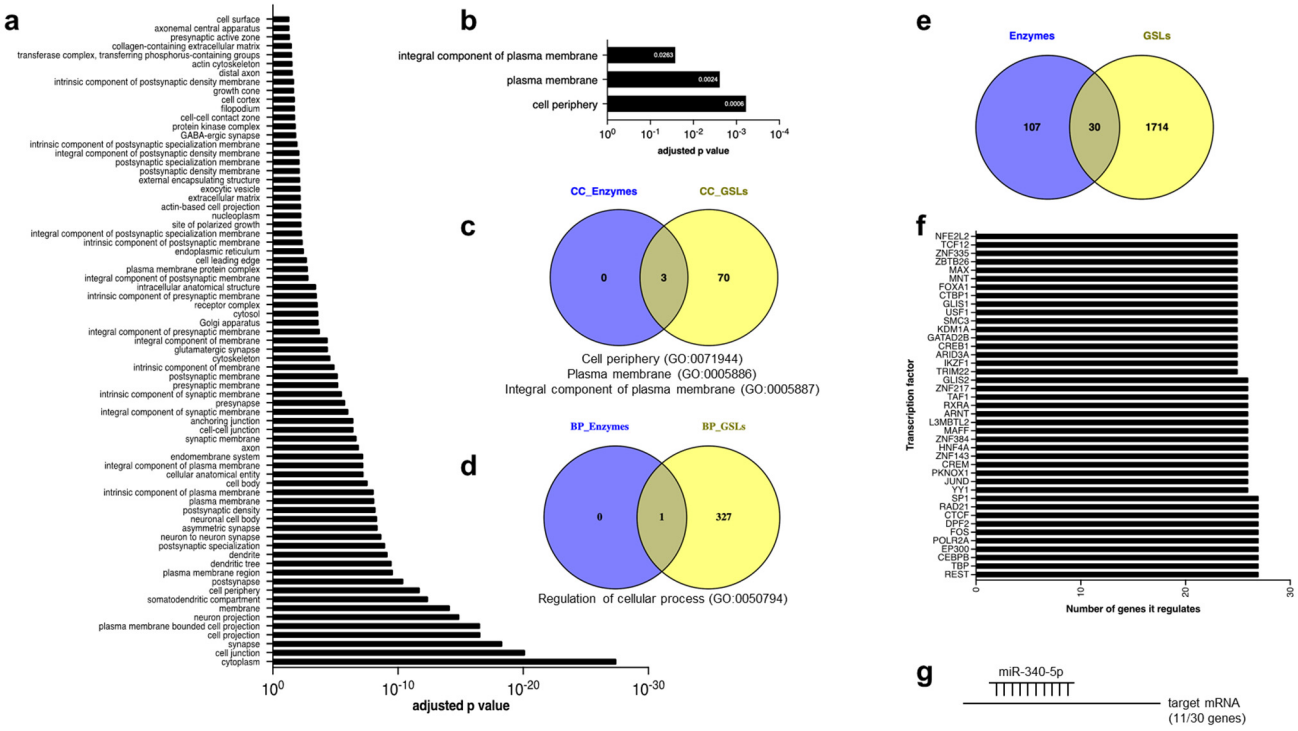

Figure 7. Enrichment analysis and common modifier genes between glycosphingolipids levels and lysosomal enzyme activities. (**a**) Cellular component functional enrichment analysis for gene sets (1744 non−redundant genes) of six substrate (GM3−Gc, GA2, Lac, GM1b, GD1b, GD1a), analyzed by g:Profiler. We found 73 GO_CC associated. (**b**) Cellular component functional enrichment analysis for gene sets (137 non−redundant genes) of eight enzymes (acid β−glucosidase, α−galactosidase A, α−galactosidase B, α−glucosidase, β−D−galactosidase, chitotriosidase, α−L−fucosidase, tartrate−resistant acid phosphatase). (**c**) Venn diagram with common GO terms cellular component between two traits. (**d**) Common GO terms biological processes between two traits. (**e**) Common genetic regulators between two traits. (**f**) Transcription factors that bind to the common genes. (**g**) Cartoon with common genetic regulators that miR−340−5p can bind.

2.9. Common and Uncommon Modifiers between Hepatic Lysosomal Enzyme Activity and Sphingolipids Levels

Common regulators of GSLs and enzymatic activities are relevant for understanding GSL metabolism and may be attractive therapeutic targets for LSDs. Therefore, we examined the overlap between them. We found 30 common and 1821 uncommon genes (Figure 7e). We explored their functions and identified genes involved in mitochondrial biogenesis and dynamics (Tfb1m, Timen135, Chchd6) [29,36,37], cell proliferation (Fstl5, Fzd10, Arhgap18) [38–40], platelet function (Cdh6) [41], vesicular trafficking (Vps45) [42], gene expression (Tfb1m, Zfat) [36,43], and regulating levels of the proto-oncogene MYC (Pvt1) [44]. Many of the 30 genes have been linked to diseases, such as Pvt1, Tiam2, Fstl5, Fzd10, Cdh6, Pvt1, Chchd6 in liver, colorectal, nasopharyngeal, and gastric cancer [45–50].

Others participate in neurodegenerative conditions; PD, schizophrenia, and intellectual disability (Tenm4, Pde4dip, Grid2, Arhgap18) [51,52]. These results suggest that lysosomal enzymes and GSLs may play a role in their pathophysiology and should be explored further (Table 2).

To better understand the molecular regulation of these 30 genes, we analyzed the transcription factors that bind to their promoters and/or enhancers (Figure 7f). We found no information for three of the 30 genes since they are putative (Rik) genes. The following transcription factors can bind to the 27 genes for which we have information: REST, TBP, CEBPB, EP300, POLR2A, FOS, DPF2, CTCF, RAD21, and SP1. Some of these transcription factors are broad regulators of transcription, such as TBP and POLR2A, while others are selective for specific processes, such as CTCF and RAD21. Considering all the promoters/enhancers of the 27 shared genes, we identified a total of 533 transcription factors that can bind them, although some only bind a few genes (Supplementary Table S6). We also searched for potential shared microRNA (miRNA) regulators using miRTarBase, a curated microRNA database [53]. We identified that miR-340-5p can bind to 11 of the 27 known common genes (Tusc1, Fam91a1, Zc3h12c, Adamts5, Tmem135, Tenm4, Grid2, Csnk1g3, Cdh6, Fam181b, and Pde4dip; $p = 2.2 \times 10^{-2}$) (Figure 7g). This result suggests that miRNA-340-5p regulates GSLs metabolism and may be involved in the pathogenesis of LSDs and the disorders described in Table 2.

Table 2. Common genetic modifiers associated with enzyme activity and hepatic glycosphingolipid levels in inbred mouse strains. The references related to this table are presented as supplementary material.

Gene	Description	Traits				Related Functions	Associated Human Diseases	Previosly Associated with Traits	References
		Enzyme	*p*-Value GWAS	GSLs	*p*-Value GWAS				
Tiam2	T cell lymphoma invasion and metastasis 2	α-Glucosidase	1.89×10^{-6}	GM3-Gc	1.51×10^{-31}	neuroplasticity	liver cancer	No	[47,54]
Tfb1m	Dimethyladenosine transferase 1, mitochondrial	α-Glucosidase	1.89×10^{-7}	GM3-Gc	1.51×10^{-31}	promotion of mitochondrial biogenesis	deafness	No	[36,55]
Dok5	Insulin receptor substrate 6	β-D-galactosidase	1.43×10^{-7}	Lac	1.38×10^{-12}	osteoblast differentiation, insulin and IGF-1 signaling	cancer, Alzheimer's disease	No	[56–59]
4930433b08Rik	RIKEN cDNA 4930433B08 gene	β-D-galactosidase	2.32×10^{-8}	Lac	1.38×10^{-12}	-	-	-	-
A830019l24Rik	RIKEN cDNA A830019L24 gene	β-D-galactosidase	1.43×10^{-7}	Lac	1.38×10^{-12}	-	-	-	-
Tmem135	Transmembrane protein 135	β-D-galactosidase	1.43×10^{-7}	GM3-Gc	1.51×10^{-31}	involved in mitochondrial dynamics	retinal diseases	No	[37,60]
Fam181b	Family with sequence similarity 181, member B	β-D-galactosidase	1.43×10^{-7}	GM3-Gc	1.51×10^{-31}	increased expression during mouse development	-	No	[31]
Tenm4	Teneurin transmembrane protein 4	β-D-galactosidase	1.43×10^{-7}	GM3-Gc	1.51×10^{-31}	cell maturation and myelination in SNC	neuropsychiatric disorders, Parkinson's disease	No	[51,61–63]
Plk2	Serine/Threonine-protein kinase PLK2	α-L-Fucosidase	1.43×10^{-7}	GM3-Gc	1.51×10^{-31}	cell proliferation, alpha-synuclein phosphorylation	pulmonary fibrosis	No	[64,65]
Stk32a	Serine/Threonine kinase 32A	α-L-Fucosidase	1.43×10^{-7}	GM3-Gc	1.51×10^{-31}	kinase activity	lung cancer	No	[66,67]
Dpysl3	Dihydropyrimidinase like 3	α-L-Fucosidase	1.43×10^{-7}	GM3-Gc	1.51×10^{-31}	cell migration, cytoskeletal dynamics and inflammation	gastric cancer, amyotrophic lateral sclerosis	No	[68–70]
Prex1	PIP3 Dependent rac exchange factor 1	α-L-Fucosidase	6.67×10^{-8}	GM3-Gc	1.51×10^{-31}	contributes to the effector activity of mouse neutrophils	prostate cancer	No	[71,72]
Fstl5	Follistatin-related protein 5	α-L-Fucosidase	6.67×10^{-8}	Lac	1.38×10^{-12}	play a role in cell proliferation	hepatocellular carcinoma	No	[38,73]
Vps45	Vacuolar protein sorting-associated protein 45	α-L-Fucosidase	1.13×10^{-1}	GM3-Gc	1.51×10^{-31}	vesicle-mediated protein trafficking from the Golgi	neutrophil disorders	No	[42,74]
Hist2h2be	Histone cluster 2 H2B family member E	α-L-Fucosidase	1.13×10^{-1}	GM3-Gc	1.51×10^{-31}	is necessary for proliferation	breast cancer	No	[75]
Pde4dip	Phosphodiesterase 4D interacting protein	α-L-Fucosidase	2.29×10^{-7}	GM3-Gc	1.51×10^{-31}	cAMP-dependent pathway to Golgi and/or centrosomes	schizophrenia	No	[52]
Tusc1	Tumor suppressor candidate 1	α-L-Fucosidase	6.67×10^{-8}	GM3-Gc	1.51×10^{-31}	reduced cell proliferation in vitro *e in vivo*	glioblastoma	No	[76,77]
Fzd10	Frizzled class receptor 10	α-L-Fucosidase	6.67×10^{-8}	GM3-Gc	1.51×10^{-31}	promotes cell proliferation through Wnt1	cancer	No	[39,48]

Table 2. *Cont.*

Gene	Description	Traits				Related Functions	Associated Human Diseases	Previosly Associated with Traits	References
		Enzyme	*p*-Value GWAS	GSLs	*p*-Value GWAS				
Grid2	Glutamate ionotropic receptor delta type subunit 2	α-L-Fucosidase	6.67×10^{-8}	Lac	1.38×10^{-12}	receptor for glutamate	neurodevelopmental syndrome/ intellectual disability	No	[78]
Zc3h12c	Zinc finger CCCH-type containing 12C	α-L-Fucosidase	1.64×10^{-6}	GM3-Gc	1.51×10^{-31}	RNA stability associated with inflammatory genes	psoriasis	No	[79,80]
Arhgap18	Rho GTPase activating protein 18	α-L-Fucosidase	6.67×10^{-8}	GM3-Gc	1.51×10^{-31}	role in migration, spreading and controls stress fiber formation	schizophrenia in Chinese population	No	[40,81]
Cdh6	Cadherin 6	α-L-Fucosidase	1.34×10^{-6}	Lac	1.38×10^{-12}	inhibit platelet aggregation	cancer	No	[41,49]
Fam91a1	Family with sequence similarity 91 member A1	α-L-Fucosidase	6.67×10^{-8}	GM3-Gc	1.51×10^{-31}	WDR11 complex (vesicular trafficking)	adenocarcinoma	No	[82,83]
4933412e24Rik	RIKEN cDNA 4933412E24 gene	α-L-Fucosidase	6.67×10^{-8}	Lac	1.38×10^{-12}	-	-	-	-
A1bg	Alpha−1B-Glycoprotein	α-L-Fucosidase	6.67×10^{-8}	GM3-Gc	1.51×10^{-31}	cell dynamics and acquired immune response	cervical and bladder carcinogenesis	No	[84–86]
Pvt1	Pvt1 Oncogene	α-L-Fucosidase	6.67×10^{-8}	GM3-Gc	1.51×10^{-31}	promotes cell proliferation	cancer	No	[50,87]
Adamts5	ADAM Metallopeptidase with thrombospondin type 1 motif 5	α-L-Fucosidase	6.67×10^{-8}	GM3-Gc	1.51×10^{-31}	metalloproteinase that remoldels connective tissue	osteoarthritis	No	[88]
Csnk1g3	Casein kinase 1 gamma 3	α-L-Fucosidase	3.51×10^{-7}	Lac	1.38×10^{-12}	wnt signaling pathway	breast, brain and colon cancer	No	[89,90]
Chchd6	Coiled-coil-helix-coiled-coil-helix domain containing 6	Chitotriosidase	1.37×10^{-6}	GA2	3.27×10^{-6}	mitochondrial membrane morphology	cancer	No	[29]
Zfat	Zinc finger protein ZFAT	TRAP	7.72×10^{-7}	Lac	1.38×10^{-12}	immune response	hashimoto's disease	No	[43,91]

3. Discussion

In this study we searched for genetic modulators involved in the regulation of the lysosomal enzyme activities and the levels of substrates related to GSLs, with the idea of finding novel therapeutics targets for disorders in which they participate. By GWASs, we identified common and uncommon genetic regulators, evaluated the associations between modifier gene mRNA levels and each trait, and also clustered them in pathways. We identified 30 shared putative modifiers and described the transcription factors that are predicted to regulate them, and we noted that the miRNA340-5p can bind to 11 of these genes.

Our first unexpected finding was that most lysosomal enzyme activities do not correlate with their mRNA levels, nor with most of their substrate levels. Although enzyme activity can decrease with age [92], we used sex and age-matched samples; thus, the variation observed across strains was shown not to be due to any of these factors.

Another unexpected finding was that GM2-Gc levels correlate with the mRNA levels of the *Cgt* gene, which encodes for the UDP-galactose ceramide galactosyltransferase (CGT). CGT is a key enzyme for the biosynthesis of galactocerebrosides. Gangliosides, including GM2 derivates, are built from glucosylceramide and not from the galacto series [93]. However, for most of the biosynthetic genes there were no associations between the amount of lipids and the transcript levels of their anabolic pathways. Altogether, our results suggest that the GSL biosynthesis rate and uptake differ across the mouse strains, suggesting the existence of specific modifier genes for each trait.

Our third unexpected finding was that TFEB, the master transcriptional regulator of lysosomal genes [94], did not appear in the list of modifiers of lysosomal enzymes. This may be due to the fact that we screened for enzymatic activity instead of mRNA levels, and we showed a lack of correlation between transcript levels and enzyme activity under physiological conditions, at least for most enzymes. One exception was β-D-galactosidase, for which we found a positive correlation between its transcript levels and activity. Furthermore, the GWAS for this enzyme identified *Glb1*, the gene encoding for β-D-galactosidase, as a

putative modifier of its activity, validating the power of discovery of our population-based strategy [95].

Our study had some limitations: First, we quantified lysosomal traits from liver homogenates that were not in living or isolated organelles, which may have diluted enzyme activity or promoted molecular interactions that might not occur in vivo because of cellular compartmentalization. Second, we could not directly measure GSLs biosynthesis and uptake because we started with mouse liver samples. Third, we used SNV catalogs with imputation, which may lead to false associations, though with increased mapping resolution.

Most of the enzymes we assayed are associated with LSDs [5,8]. For many LSDs, no therapies are available, and the few currently available treatments have severe limitations [5]. In this context, targeting a modifier gene could be a novel therapeutic approach. For example, lack of β-D-galactosidase activity triggers GM1 gangliosidosis, a disease with no approved therapies [96]. Our study identified the druggable *Lypla1* and *Pkm* genes as putative modifiers of β-D-galactosidase activity, which can be pharmacologically modulated [97,98]. We found other druggable genes as well for several traits, and with the current gene editing technologies virtually any gene can be targeted. The potential modifying effects of these genes and compounds can be tested in LSDs disease models.

A hallmark of the sphingolipidoses is the intracellular buildup of GSLs, so strategies aimed at reducing their levels could lead us to novel therapies [5,8]. GSLs comprise a ceramide moiety with one or more sugar residues linked to it [99]. An approved therapy for Gaucher and Niemann-Pick disease type C is Miglustat [100,101], a small molecule inhibitor of GSL biosynthesis, thus reducing their levels. Our GSLs GWAS identified more than 50 genes previously associated with sphingolipid metabolism, which served as a positive control, including *B3gnt5, Cln8, Hexb, Pnpla1, St8sia1*, and *Cgt. B3gnt5* regulates GSLs metabolism and lung tumorigenesis [102]. Our study also identified *Lipc* as a modifier of GM3-Gc levels, which has been previously associated with elevated serum levels of liver enzymes (alkaline phosphatase and γ-glutamyl transferase) [103], suggesting a new connection between GM3-Gc and liver damage. Variants in *LIPC, CPS1, PABPC4, CITED2, TRPS1,* and *MVK* are associated with changes in plasma lipoprotein levels [104], connecting novel traits to GSLs metabolism.

Lysosomal leakage has been associated with Alzheimers' [105], cancer, and inflammation among other conditions [106]. Recently, the phosphoinositide signaling pathway was implicated in lysosomal repair [107]. Many genes of this pathway appear in our discovery list (*Osbpl9, Osbpl6, Pde4dip, Pde2a, Pde1a, Pde7a, Pde7b, Pde4d, Pde8b, Pld5, Pik3r1, Pip4k2a, Pip5k1a, Pip5k1b, Pi4kb, Pdpk1, Atg4c, Atg10*), suggesting that integrity of the lysosomal compartment is key to the proper functioning of enzymes and/or that these enzymes and lipids participate in lysosomal repair. Furthermore, this novel lysosomal repair pathway may facilitate the development of novel therapeutics for these diseases with lysosomal leakage.

Defects in the 30 shared genes are related to several pathologies, such as vision abnormalities (*TMEM135*) [60], cancer (*CDH6* [49], *FZD10* [48], *TIAM2* [47]), neuropsychiatric disorders (*Tenm4* [51], *Pde4dip* [52], *Grid2* [78]), deafness (*TFB1M*) [55], neutrophil disorders (*VPS45*) [74] and others. Lysosomal enzymes and GSLs have been widely studied in cancer and neurodegenerative diseases [46,108–111]; however, their role in the other identified conditions should be explored.

Although not binding the complete list of shared genes, we identified some transcription factors previously known to be involved in lipid metabolism and autophagy-lysosomal functions (PPARγ, SREBF1, HNF1A, YY1, EGR1, SP1 and TFE3, E2F1, CREB1, MYC) [112–121], and many more that have not been previously linked to GSL metabolism. We also identified miR-340-5p as a putative regulator of many common modifier genes. Changes in miR-340-5p are linked to preeclampsia, neuroinflammation [122–126], adipocyte differentiation [127], as well as obesity and diabetes [128]. GSL metabolism plays a crucial role in the two last-mentioned disorders, and inhibitors of their biosynthesis have shown

promising results in animal models of these conditions, validating the relevance of our strategy [129,130].

In conclusion, we described putative regulators of hepatic lysosomal enzymes and GSLs, many of them druggable and associated with diseases where alterations in GSL metabolism have not been previously described and should be assessed. We expect our findings may facilitate the development of novel therapeutics for conditions with alterations in these traits.

4. Materials and Methods

4.1. Mouse Tissues

We used 8 weeks-old mice livers derived from 25 inbred mouse strains, which were kindly donated by Dr. Aldons Lusis (University of California, Los Angeles, CA, USA). (i) 129X1/SvJ, (ii) A/J, (iii) AKR/J, (iv) BALB/cJ, (v) BTBR T<+> tf/J, (vi) BUB/BnJ, (vii) C57BL/6J, (viii) C58/J, (ix) CAST/EiJ, (x) CBA/J, (xi) CE/J, (xii) DBA/2J, (xiii) KK/HlJ, (xiv) LG/J, (xv) LP/J, (xvi) MA/MyJ, (xvii) NOD/ShiLtJ, (xviii) NON/ShiLtJ, (xix) NZB/BlNJ, (xx) NZW/LacJ, (xxi) PL/J, (xxii) RIIIS/J, (xxiii) SEA/GnJ, (xxiv) SM/J, (xxv) SWR/J. Tissues were homogenized and adjusted to 50 mg tissue/mL in deionized water with a Potter-Elvehjem tissue homogenizer (Omni International, Kennesaw, GA, USA). Three or more livers per mouse strain were used to quantify traits (Supplementary Table S7).

4.2. Enzyme Activity Assays

Lysosomal hydrolase activities were determined using an artificial fluorescent substrate based on 4-methylumbelliferone (4-MU) [131]. For α-glucosidase, 1.47 mM 4-MU α-D-glucopyranoside (Sigma, Dorset, UK) in 100 mM citric acid/100 mM sodium phosphate, 0.1% TritonX-100, pH 4.0 was used as substrate [132]. The substrate for α-galactosidase A and B activities was 5 mM 4-MU α-D-galactopyranoside (Santa Cruz, CA, USA) with and without 250 mM N-acetyl-galactosamine (Sigma, Dorset, UK) in 100 mM citric acid/100 mM tri-sodium citrate, 0.1% TritonX-100, pH 4.0 [133,134]. For measuring β-hexosaminidase A and B activity, 3 mM 4-MU N-acetyl-β-D-glucosaminide (BioChemika, Dorset, UK) in 100 mM citric acid/100 mM sodium phosphate, 0.1% TritonX-100, pH 4.5 was used as substrate. Heat inactivation assay for β-hexosaminidase A was carried out at 50 °C for 3 h [135]. For β-galactosidase activity, 1 mM 4-MU β-D-galactose (Sigma, Dorset, UK) in 200 mM sodium acetate buffer, 100 mM NaCl, 0.1% TritonX-100, pH 4.3 was used as substrate [136]. The substrate for neuraminidase activity was 0.4 mM 4-MU α-D-N-acetylneuraminic acid (Sigma, Dorset, UK) in 0.1 M acetate buffer, 0.1% TritonX-100, pH 4.6 [137,138]. For chitotriosidase activity, 0.013 mM 4-MU chitotrioside (Sigma, Dorset, UK) in 100 mM citric acid/200 mM sodium phosphate, 0.1% TritonX-100, pH 5.2 was used as substrate [139,140]. For total acid phosphatase activity, 5 mM 4-MU phosphate (Sigma, Dorset, UK) with 40 mM NaCl in 200 mM citric acid/200 mM sodium phosphate, 0.1% TritonX-100, pH 4.5 was used as substrate. For tartrate-resistant acid phosphatase (TRAP) activity, 5 mM 4-MU phosphate (Sigma, Dorset, UK) with 40 mM Na Tartrate in 200 mM citric acid/200 mM sodium phosphate, 0.1% TritonX-100, pH 4.5 was used as substrate. The difference between total acid phosphatase activity and TRAP corresponded to lysosomal acid phosphatase (Lys AP) activity [141,142]. The substrate for α-L-fucosidase activity was 60 nM 4-MU α-L-fucopyranoside (Sigma, Dorset, UK) in 200 mM citric acid/200 mM sodium citrate, 0.1% TritonX-100, pH 5.0 [143,144]. We determined the acid-β-glucosidase activity in the same tissues in a previous publication [20], and further analyses were performed here based on the published activity. Liver homogenates were diluted with the buffer corresponding to each enzymatic determination. Three cycles of freezing (liquid nitrogen) and thawing were performed on the samples. Three biological replicates of the diluted liver extracts were incubated with the corresponding substrate at 37 °C for 30 min (or 1 h for α-neuraminidase, β-D-galactosidase, and chitotriosidase). Cold 0.5 M Na_2CO_3 (pH 10.7) was added to stop the reaction. Fluorescence intensity in samples was measured in a Synergy HT plate reader (BioTek, Winooski, VT, USA) at 360/460 nm. Protein concentration

was measured using a BCA protein assay kit (Thermo Fisher Scientific, New Jersey, NJ USA). Fluorescence values were normalized to protein concentration. A 4-MU standard curve was constructed to calculate specific activity, and the final value was adjusted to one hour of enzymatic reaction.

4.3. Glycosphingolipids Levels Quantification

The GSLs were extracted and measured by Normal Phase-High-Performance Liquid Chromatography (NP-HPLC) following published methods [145]. Briefly, the aqueous tissue extract was homogenized in chloroform/methanol (C:M) (1:2 v/v) and kept overnight at 4 °C. Then, the extracts mixture was centrifuged at 3000 rpm for 10 min at room temperature. We added 0.5 mL of PBS and 0.5 mL of chloroform to the supernatant followed by a 3000-rpm centrifugation for 10 min at room temperature. The lower phase was carefully removed and dried under a stream of nitrogen gas (N2) in a heating block (42 °C), resuspended in 40 µL C:M 1:3 v/v and mixed with the upper phase. Afterwards, glycosphingolipids-derived oligosaccharides were purified from the samples using C18 columns (Telos, Kinesis, UK) previously pre-equilibrated with 1.25 mL methanol (four times) and 1.25 mL deionized water (three times). We loaded the mixed phase (lower/upper) onto a column and rinsed the sample tube with 1 × 1 mL of deionized water. Then, the C18 column was washed with 4 × 1.25 mL deionized water and eluted it with 1 × 1 mL (C:M) (98:2 v/v), 2 × 1 mL (C:M) (1:3 v/v), 1 × 1 mL methanol. The eluates were dried under N2 current and digested with a recombinant Endoglycoceramidase I (rEGCaseI) (GenScript, Oxford, UK) in buffer 50 mM sodium acetate, pH 5.0, 0.6% TritonX-100 (4 µL enzyme + 86 µL buffer) at 37 °C for 16 h. The released glycans were labeled with 310 µL of labelling mix (30 mg/mL anthranilic acid (2AA) and 45 mg/mL sodium cyanoborohydride) in 4% sodium acetate, 2% boric acid in methanol, and heated at 80 °C. Then, we cooled the samples and mixed them with 3 × 1 mL acetonitrile: deionized water (97:3) (v/v) and added them to a Discovery DPA-6S-SPE tube (Supelco, PA, USA), pre-equilibrated with 1 × 1 mL acetonitrile, 2 × 1 mL deionized water, and 3 × 1 mL acetonitrile. The columns were cleaned with 3 × 1 mL acetonitrile: deionized water (95:5) (v/v), and the tubes were washed with 2 × 1 mL acetonitrile: deionized water (95:5) (v/v) and eluted in 0.6 mL deionized water. We took 60 µL from 0.6 mL sample eluted, added 140 µL acetonitrile, and injected 50 µL of this mix (deionized water: acetonitrile) (30:70) (v/v) onto NP-HPLC (Waters Alliance 2695 separations module and multi-fluorescent detector set at Ex 360/Em 425 nm). To calculate molar quantities from peaks in the chromatogram, we included a calibration standard containing 2.5 pmol 2AA-labelled chitotriose (Ludger, Oxford, UK) for each NP-HPLC run [145]. The chromatographic data were processed using Waters Empower software 3 (Waters, Milford, MA, USA). Fluorescence values by sample were normalized to protein content using a BCA Assay kit (Merck KGaA, Darmstadt, Germany).

4.4. Genome-Wide Association Studies (GWAS)

We used the genotype of each strain, and the enzymatic activity or substrate as trait, and its kinship matrix to perform the GWAS using The Efficient Mixed Model Association (EMMA) v.1.1.230 in the R package [26,146]. We used PLINK to remove SNVs in linkage disequilibrium to avoid false associations [25], considering an R^2 = 0.25, leaving 127,285 independent variants out of the initial four million variants downloaded from the mouse HapMap reference panel (http://mouse.cs.ucla.edu/mousehapmap/full.html, accessed on 28 September 2020) [147].

4.5. Gene Expression Array and Heat Maps

For gene expression correlations, we obtained inbred mouse hepatic transcript data from the repository GSE16780 UCLA Hybrid MDP Liver Affy HTM430A [24]. The mRNA levels in the repository were expressed as log2 transformed and were calculated from the Affimetrix chip with the robust multiarray average (RMA) method. To plot the heatmaps,

we used Morpheus software (https://software.broadinstitute.org/morpheus, accessed on 15 February 2022).

4.6. Functional Impact of Genomic Variants

The functional impact of genomic variants was assessed using the Sorting Intolerant From Tolerant (SIFT) software (https://sift.bii.a-star.edu.sg/www/SIFT_dbSNP.html, accessed on 12 July 2022) [27].

4.7. Enrichment Analysis

We used gProfiler [35] with the default settings to perform the pathway enrichment analyses.

4.8. Identification of Transcription Factors

We consulted the GeneHancer (GH) database, a catalogue of genome-wide enhancer-to-gene and promoter-to-gene associations, through GeneCards® (https://www.genecards.org/Guide/GeneCard, accessed on 6 September 2022) [148]. Only transcription factors with a significative GH Score were considered.

4.9. Statistics

We used Student's *t*-test, ANOVA with Bonferroni correction, and Pearson correlation. All tests were two-tailed. The significance was considered to be $p < 0.05$. We used an R package [146] and Prism v9.1.0 (GraphPad software, San Diego, CA, USA) for these analyses.

Supplementary Materials: The following supporting information can be downloaded at: https://www.mdpi.com/article/10.3390/ijms24054915/s1.

Author Contributions: Conceptualization, A.D.K.; methodology, A.D., D.A.P. and V.O.; bioinformatics analyses, A.D., B.R.-J., M.L.H. and J.F.C.; writing—original draft preparation, A.D. and A.D.K.; writing—review and editing, all the authors.; supervision, J.F.C., S.Z., J.G., F.M.P. and A.D.K.; funding acquisition, D.A.P., S.Z., F.M.P. and A.D.K. All authors have read and agreed to the published version of the manuscript.

Funding: This work was supported by ANID-CHILE: Fondecyt grant No 1180337 (A.D.K.) (2018–2022), 1190334 (S.Z.) (2019–2023), EQM190110 and ACT210012 (J.F.C.), EQM150093 (B.R.-J.) and 1221362 (J.G.) (2022–2025). LysoMod, funded by the European Union's Horizon 2020 research and innovation programme (RISE) under the Marie Sklodowska-Curie grant agreement No 734825 (S.Z., F.M.P., A.D.K.) (2017–2022), and the Mizutani Foundation for Glycoscience, grant No: 200133 (F.M.P., D.A.P., A.D.K.) (2020). F.M.P. is a Wolfson Royal Society Merit Award Holder and a Wellcome Trust Investigator in science.

Institutional Review Board Statement: The animal study protocol was approved by the Institutional Review Board of Universidad del Desarrollo (protocol code number 04-2018 approved on 4 June 2018).

Informed Consent Statement: Not applicable.

Data Availability Statement: We obtained inbred mouse hepatic transcript data from the repository GSE16780 UCLA Hybrid MDP Liver Affy HTM430A reported in [24].

Acknowledgments: The authors thank Aldons J. Lusis from University of California Los Angeles (UCLA) for donating the mouse tissues and María E. Fernández-Suárez and Rodrigo Escalona-Rivano for technical support.

Conflicts of Interest: The authors declare no conflict of interest.

References

1. Mosen, P.; Sanner, A.; Singh, J.; Winter, D. Targeted Quantification of the Lysosomal Proteome in Complex Samples. *Proteomes* **2021**, *9*, 4. [CrossRef] [PubMed]
2. Brubaker, P.L.; Martchenko, A. Metabolic Homeostasis: It's All in the Timing. *Endocrinology* **2021**, *163*, bqab199. [CrossRef] [PubMed]
3. Settembre, C.; Fraldi, A.; Medina, D.L.; Ballabio, A. Signals from the lysosome: A control centre for cellular clearance and energy metabolism. *Nat. Rev. Mol. Cell Biol.* **2013**, *14*, 283–296. [CrossRef]
4. Ballabio, A.; Bonifacino, J.S. Lysosomes as dynamic regulators of cell and organismal homeostasis. *Nat. Rev. Mol. Cell Biol.* **2019**, *21*, 101–118. [CrossRef]
5. Platt, F.M.; D'Azzo, A.; Davidson, B.; Neufeld, E.F.; Tifft, C.J. Lysosomal storage diseases. *Nat. Rev. Dis. Prim.* **2018**, *4*, 27. [CrossRef] [PubMed]
6. Sidransky, E.; Nalls, M.; Aasly, J.; Aharon-Peretz, J.; Annesi, G.; Barbosa, E.; Bar-Shira, A.; Berg, D.; Bras, J.; Brice, A.; et al. Multicenter Analysis of Glucocerebrosidase Mutations in Parkinson's Disease. *N. Engl. J. Med.* **2009**, *361*, 1651–1661. [CrossRef] [PubMed]
7. Klein, A.D.; Mazzulli, J.R. Is Parkinson's disease a lysosomal disorder? *Brain* **2018**, *141*, 2255–2262. [CrossRef]
8. Platt, F.M. Sphingolipid lysosomal storage disorders. *Nature* **2014**, *510*, 68–75. [CrossRef]
9. Jeyakumar, M.; Butters, T.D.; Cortina-Borja, M.; Hunnam, V.; Proia, R.L.; Perry, V.H.; Dwek, R.A.; Platt, F.M. Delayed symptom onset and increased life expectancy in Sandhoff disease mice treated with *N*-butyldeoxynojirimycin. *Proc. Natl. Acad. Sci. USA* **1999**, *96*, 6388–6393. [CrossRef]
10. Peterschmitt, M.J.; Crawford, N.P.S.; Gaemers, S.J.M.; Ji, A.J.; Sharma, J.; Pham, T.T. Pharmacokinetics, Pharmacodynamics, Safety, and Tolerability of Oral Venglustat in Healthy Volunteers. *Clin. Pharmacol. Drug Dev.* **2020**, *10*, 86–98. [CrossRef]
11. Kan, S.-H.; Aoyagi-Scharber, M.; Le, S.Q.; Vincelette, J.; Ohmi, K.; Bullens, S.; Wendt, D.J.; Christianson, T.M.; Tiger, P.M.N.; Brown, J.R.; et al. Delivery of an enzyme-IGFII fusion protein to the mouse brain is therapeutic for mucopolysaccharidosis type IIIB. *Proc. Natl. Acad. Sci. USA* **2014**, *111*, 14870–14875. [CrossRef] [PubMed]
12. Weesner, J.A.; Annunziata, I.; Yang, T.; Acosta, W.; Gomero, E.; Hu, H.; van de Vlekkert, D.; Ayala, J.; Qiu, X.; Fremuth, L.E.; et al. Preclinical Enzyme Replacement Therapy with a Recombinant β-Galactosidase-Lectin Fusion for CNS Delivery and Treatment of GM1-Gangliosidosis. *Cells* **2022**, *11*, 2579. [CrossRef] [PubMed]
13. Sevin, C.; Deiva, K. Clinical Trials for Gene Therapy in Lysosomal Diseases With CNS Involvement. *Front. Mol. Biosci.* **2021**, *8*, 624988. [CrossRef]
14. Hobbs, J. reversal of clinical features of hurler's disease and biochemical improvement after treatment by bone-marrow transplantation. *Lancet* **1981**, *318*, 709–712. [CrossRef]
15. Dever, D.P.; Scharenberg, S.G.; Camarena, J.; Kildebeck, E.J.; Clark, J.T.; Martin, R.M.; Bak, R.O.; Tang, Y.; Dohse, M.; Birgmeier, J.A.; et al. CRISPR/Cas9 Genome Engineering in Engraftable Human Brain-Derived Neural Stem Cells. *Iscience* **2019**, *15*, 524–535. [CrossRef] [PubMed]
16. Kirkegaard, T.; Gray, J.; Priestman, D.A.; Wallom, K.-L.; Atkins, J.; Olsen, O.D.; Klein, A.; Drndarski, S.; Petersen, N.H.T.; Ingemann, L.; et al. Heat shock protein–based therapy as a potential candidate for treating the sphingolipidoses. *Sci. Transl. Med.* **2016**, *8*, 355ra118. [CrossRef]
17. Wraith, J.E. Limitations of enzyme replacement therapy: Current and future. *J. Inherit. Metab. Dis.* **2006**, *29*, 442–447. [CrossRef]
18. Broomfield, A.; Jones, S.; Hughes, S.M.; Bigger, B. The impact of the immune system on the safety and efficiency of enzyme replacement therapy in lysosomal storage disorders. *J. Inherit. Metab. Dis.* **2016**, *39*, 499–512. [CrossRef]
19. Richardson, J.S.; Kemper, A.R.; Grosse, S.D.; Lam, W.K.K.; Rose, A.M.; Ahmad, A.; Ms, A.G.; Prosser, L.A. Health and economic outcomes of newborn screening for infantile-onset Pompe disease. *Anesthesia Analg.* **2020**, *23*, 758–766. [CrossRef]
20. Durán, A.; Rebolledo-Jaramillo, B.; Olguin, V.; Rojas-Herrera, M.; Heras, M.L.; Calderón, J.F.; Zanlungo, S.; Priestman, D.A.; Platt, F.M.; Klein, A.D. Identification of genetic modifiers of murine hepatic β-glucocerebrosidase activity. *Biochem. Biophys. Rep.* **2021**, *28*, 101105. [CrossRef]
21. Ferland, R.J.; Smith, J.; Papandrea, D.; Gracias, J.; Hains, L.; Kadiyala, S.B.; O'Brien, B.; Kang, E.Y.; Beyer, B.S.; Herron, B.J. Multidimensional Genetic Analysis of Repeated Seizures in the Hybrid Mouse Diversity Panel Reveals a Novel Epileptogenesis Susceptibility Locus. *G3 Genes Genomes Genet.* **2017**, *7*, 2545–2558. [CrossRef] [PubMed]
22. Klein, A.D.; Ferreira, N.-S.; Ben-Dor, S.; Duan, J.; Hardy, J.; Cox, T.M.; Merril, A.H., Jr.; Futerman, A.H. Identification of Modifier Genes in a Mouse Model of Gaucher Disease. *Cell Rep.* **2016**, *16*, 2546–2553. [CrossRef]
23. Ghazalpour, A.; Rau, C.D.; Farber, C.R.; Bennett, B.J.; Orozco, L.D.; Van Nas, A.; Pan, C.; Allayee, H.; Beaven, S.W.; Civelek, M.; et al. Hybrid mouse diversity panel: A panel of inbred mouse strains suitable for analysis of complex genetic traits. *Mamm. Genome* **2012**, *23*, 680–692. [CrossRef] [PubMed]
24. Bennett, B.J.; Farber, C.R.; Orozco, L.; Kang, H.M.; Ghazalpour, A.; Siemers, N.; Neubauer, M.; Neuhaus, I.; Yordanova, R.; Guan, B.; et al. A high-resolution association mapping panel for the dissection of complex traits in mice. *Genome Res.* **2010**, *20*, 281–290. [CrossRef]
25. Purcell, S.; Neale, B.; Todd-Brown, K.; Thomas, L.; Ferreira, M.A.R.; Bender, D.; Maller, J.; Sklar, P.; de Bakker, P.I.W.; Daly, M.J.; et al. PLINK: A Tool Set for Whole-Genome Association and Population-Based Linkage Analyses. *Am. J. Hum. Genet.* **2007**, *81*, 559–575. [CrossRef]

26. Kang, H.M.; Zaitlen, N.A.; Wade, C.M.; Kirby, A.; Heckerman, D.; Daly, M.J.; Eskin, E. Efficient Control of Population Structure in Model Organism Association Mapping. *Genetics* **2008**, *178*, 1709–1723. [CrossRef] [PubMed]
27. Vaser, R.; Adusumalli, S.; Leng, S.N.; Sikic, M.; Ng, P.C. SIFT missense predictions for genomes. *Nat. Protoc.* **2015**, *11*, 1–9. [CrossRef]
28. Keane, T.M.; Goodstadt, L.; Danecek, P.; White, M.A.; Wong, K.; Yalcin, B.; Heger, A.; Agam, A.; Slater, G.; Goodson, M.; et al. Mouse genomic variation and its effect on phenotypes and gene regulation. *Nature* **2011**, *477*, 289–294. [CrossRef]
29. An, J.; Shi, J.; He, Q.; Lui, K.; Liu, Y.; Huang, Y.; Sheikh, M.S. CHCM1/CHCHD6, Novel Mitochondrial Protein Linked to Regulation of Mitofilin and Mitochondrial Cristae Morphology. *J. Biol. Chem.* **2012**, *287*, 7411–7426. [CrossRef]
30. Verde, I.; Pahlke, G.; Salanova, M.; Zhang, G.; Wang, S.; Coletti, D.; Onuffer, J.; Jin, S.-L.C.; Conti, M. Myomegalin Is a Novel Protein of the Golgi/Centrosome That Interacts with a Cyclic Nucleotide Phosphodiesterase. *J. Biol. Chem.* **2001**, *276*, 11189–11198. [CrossRef]
31. Marks, M.; Pennimpede, T.; Lange, L.; Grote, P.; Herrmann, B.G.; Wittler, L. Analysis of the Fam181 gene family during mouse development reveals distinct strain-specific expression patterns, suggesting a role in nervous system development and function. *Gene* **2015**, *575*, 438–451. [CrossRef]
32. Li, H.; Rauch, T.; Chen, Z.-X.; Szabó, P.E.; Riggs, A.D.; Pfeifer, G.P. The Histone Methyltransferase SETDB1 and the DNA Methyltransferase DNMT3A Interact Directly and Localize to Promoters Silenced in Cancer Cells. *J. Biol. Chem.* **2006**, *281*, 19489–19500. [CrossRef] [PubMed]
33. Beaubien, F.; Raja, R.; Kennedy, T.E.; Fournier, A.E.; Cloutier, J.-F. Slitrk1 is localized to excitatory synapses and promotes their development. *Sci. Rep.* **2016**, *6*, 27343. [CrossRef] [PubMed]
34. Hannun, Y.A.; Obeid, L.M. Sphingolipids and their metabolism in physiology and disease. *Nat. Rev. Mol. Cell Biol.* **2017**, *19*, 175–191. [CrossRef]
35. Raudvere, U.; Kolberg, L.; Kuzmin, I.; Arak, T.; Adler, P.; Peterson, H.; Vilo, J. g: Profiler: A web server for functional enrichment analysis and conversions of gene lists (2019 update). *Nucleic Acids Res.* **2019**, *47*, W191–W198. [CrossRef] [PubMed]
36. Gleyzer, N.; Vercauteren, K.; Scarpulla, R.C. Control of Mitochondrial Transcription Specificity Factors (TFB1M and TFB2M) by Nuclear Respiratory Factors (NRF-1 and NRF-2) and PGC-1 Family Coactivators. *Mol. Cell. Biol.* **2005**, *25*, 1354–1366. [CrossRef] [PubMed]
37. Lee, W.-H.; Higuchi, H.; Ikeda, S.; Macke, E.L.; Takimoto, T.; Pattnaik, B.R.; Liu, C.; Chu, L.-F.; Siepka, S.M.; Krentz, K.J.; et al. Mouse Tmem135 mutation reveals a mechanism involving mitochondrial dynamics that leads to age-dependent retinal pathologies. *eLife* **2016**, *5*, e19264. [CrossRef]
38. Zhang, D.; Ma, X.; Sun, W.; Cui, P.; Lu, Z. Down-regulated FSTL5 promotes cell proliferation and survival by affecting Wnt/β-catenin signaling in hepatocellular carcinoma. *Int. J. Clin. Exp. Pathol.* **2015**, *8*, 3386–3394.
39. Alrefaei, A.F.; Münsterberg, A.E.; Wheeler, G.N. FZD10 regulates cell proliferation and mediates Wnt1 induced neurogenesis in the developing spinal cord. *PLoS ONE* **2020**, *15*, e0219721. [CrossRef]
40. Maeda, M.; Hasegawa, H.; Hyodo, T.; Ito, S.; Asano, E.; Yuang, H.; Funasaka, K.; Shimokata, K.; Hasegawa, Y.; Hamaguchi, M.; et al. ARHGAP18, a GTPase-activating protein for RhoA, controls cell shape, spreading, and motility. *Mol. Biol. Cell* **2011**, *22*, 3840–3852. [CrossRef]
41. Dunne, E.; Spring, C.M.; Reheman, A.; Jin, W.; Berndt, M.C.; Newman, D.K.; Newman, P.J.; Ni, H.; Kenny, D. Cadherin 6 Has a Functional Role in Platelet Aggregation and Thrombus Formation. *Arter. Thromb. Vasc. Biol.* **2012**, *32*, 1724–1731. [CrossRef]
42. Frey, L.; Ziętara, N.; Łyszkiewicz, M.; Marquardt, B.; Mizoguchi, Y.; Linder, M.I.; Liu, Y.; Giesert, F.; Wurst, W.; Dahlhoff, M.; et al. Mammalian VPS45 orchestrates trafficking through the endosomal system. *Blood* **2021**, *137*, 1932–1944. [CrossRef]
43. Koyanagi, M.; Nakabayashi, K.; Fujimoto, T.; Gu, N.; Baba, I.; Takashima, Y.; Doi, K.; Harada, H.; Kato, N.; Sasazuki, T.; et al. ZFAT expression in B and T lymphocytes and identification of ZFAT-regulated genes. *Genomics* **2008**, *91*, 451–457. [CrossRef]
44. Jin, K.; Wang, S.; Zhang, Y.; Xia, M.; Mo, Y.; Li, X.; Li, G.; Zeng, Z.; Xiong, W.; He, Y. Long non-coding RNA PVT1 interacts with MYC and its downstream molecules to synergistically promote tumorigenesis. *Cell. Mol. Life Sci.* **2019**, *76*, 4275–4289. [CrossRef] [PubMed]
45. Tang, T.; Yang, Z.-Y.; Wang, D.; Yang, X.-Y.; Wang, J.; Li, L.; Wen, Q.; Gao, L.; Bian, X.-W.; Yu, S.-C. The role of lysosomes in cancer development and progression. *Cell Biosci.* **2020**, *10*, 131. [CrossRef] [PubMed]
46. Davidson, S.M.; Vander Heiden, M.G. Critical Functions of the Lysosome in Cancer Biology. *Annu. Rev. Pharmacol. Toxicol.* **2017**, *57*, 481–507. [CrossRef]
47. Chen, J.-S.; Su, I.-J.; Leu, Y.-W.; Young, K.-C.; Sun, H.S. Expression of T-cell lymphoma invasion and metastasis 2 (TIAM2) promotes proliferation and invasion of liver cancer. *Int. J. Cancer* **2011**, *130*, 1302–1313. [CrossRef] [PubMed]
48. Terasaki, H.; Saitoh, T.; Shiokawa, K.; Katoh, M. Frizzled-10, up-regulated in primary colorectal cancer, is a positive regulator of the WNT—Beta-catenin—TCF signaling pathway. *Int. J. Mol. Med.* **2002**, *9*, 107–112. [PubMed]
49. Zhao, Z.; Li, S.; Li, S.; Wang, J.; Lin, H.; Fu, W. High expression of oncogene cadherin-6 correlates with tumor progression and a poor prognosis in gastric cancer. *Cancer Cell Int.* **2021**, *21*, 493. [CrossRef]
50. Cui, M.; Chang, Y.; Fang, Q.-G.; Du, W.; Wu, J.-F.; Wang, J.-H.; Liu, S.-T.; Luo, S.-X. Non-Coding RNA Pvt1 Promotes Cancer Stem Cell–Like Traits in Nasopharyngeal Cancer via Inhibiting miR-1207. *Pathol. Oncol. Res.* **2018**, *25*, 1411–1422. [CrossRef]

51. Elotan, A.; Efenckova, M.; Ebralten, J.; Ealttoa, A.; Edixson, L.; Williams, R.W.; van der Voet, M. Neuroinformatic analyses of common and distinct genetic components associated with major neuropsychiatric disorders. *Front. Neurosci.* **2014**, *8*, 331. [CrossRef]
52. Kim, S.; Cho, H.; Lee, D.; Webster, M.J. Association between SNPs and gene expression in multiple regions of the human brain. *Transl. Psychiatry* **2012**, *2*, e113. [CrossRef] [PubMed]
53. Hsu, S.-D.; Lin, F.-M.; Wu, W.-Y.; Liang, C.; Huang, W.-C.; Chan, W.-L.; Tsai, W.-T.; Chen, G.-Z.; Lee, C.-J.; Chiu, C.-M.; et al. miRTarBase: A database curates experimentally validated microRNA–target interactions. *Nucleic Acids Res.* **2010**, *39*, D163–D169. [CrossRef] [PubMed]
54. Chu, C.; Chen, J.; Chuang, P.; Su, C.; Chan, Y.-L.; Yang, Y.; Chiang, Y.; Su, Y.; Gean, P.; Sun, H.S. TIAM2S as a novel regulator for serotonin level enhances brain plasticity and locomotion behavior. *FASEB J.* **2020**, *34*, 3267–3288. [CrossRef] [PubMed]
55. Bykhovskaya, Y.; Mengesha, E.; Wang, D.; Yang, H.; Estivill, X.; Shohat, M.; Fischel-Ghodsian, N. Human mitochondrial transcription factor B1 as a modifier gene for hearing loss associated with the mitochondrial A1555G mutation. *Mol. Genet. Metab.* **2004**, *82*, 27–32. [CrossRef] [PubMed]
56. Fulzele, K.; Riddle, R.C.; DiGirolamo, D.J.; Cao, X.; Wan, C.; Chen, D.; Faugere, M.-C.; Aja, S.; Hussain, M.A.; Brüning, J.C.; et al. Insulin Receptor Signaling in Osteoblasts Regulates Postnatal Bone Acquisition and Body Composition. *Cell* **2022**, *185*, 746. [CrossRef] [PubMed]
57. Dearth, R.K.; Cui, X.; Kim, H.-J.; Kuiatse, I.; Lawrence, N.A.; Zhang, X.; Divisova, J.; Britton, O.L.; Mohsin, S.; Allred, D.C.; et al. Mammary Tumorigenesis and Metastasis Caused by Overexpression of Insulin Receptor Substrate 1 (IRS-1) or IRS-2. *Mol. Cell. Biol.* **2006**, *26*, 9302–9314. [CrossRef]
58. Ochiai, T.; Sano, T.; Nagayama, T.; Kubota, N.; Kadowaki, T.; Wakabayashi, T.; Iwatsubo, T. Differential involvement of insulin receptor substrate (IRS)-1 and IRS-2 in brain insulin signaling is associated with the effects on amyloid pathology in a mouse model of Alzheimer's disease. *Neurobiol. Dis.* **2021**, *159*, 105510. [CrossRef]
59. Xu, L.; Wu, J.; Yu, Y.; Li, H.; Sun, S.; Zhang, T.; Wang, M. Dok5 regulates proliferation and differentiation of osteoblast via ca-nonical Wnt/β-catenin signaling. *J. Musculoskelet. Neuronal Interact.* **2022**, *22*, 113–122.
60. Landowski, M.; Bhute, V.J.; Takimoto, T.; Grindel, S.; Shahi, P.K.; Pattnaik, B.R.; Ikeda, S.; Ikeda, A. A mutation in transmembrane protein 135 impairs lipid metabolism in mouse eyecups. *Sci. Rep.* **2022**, *12*, 756. [CrossRef]
61. Suzuki, N.; Fukushi, M.; Kosaki, K.; Doyle, A.D.; De Vega, S.; Yoshizaki, K.; Akazawa, C.; Arikawa-Hirasawa, E.; Yamada, Y. Teneurin-4 Is a Novel Regulator of Oligodendrocyte Differentiation and Myelination of Small-Diameter Axons in the CNS. *J. Neurosci.* **2012**, *32*, 11586–11599. [CrossRef] [PubMed]
62. Pu, J.-L.; Gao, T.; Si, X.-L.; Zheng, R.; Jin, C.-Y.; Ruan, Y.; Fang, Y.; Chen, Y.; Song, Z.; Yin, X.-Z.; et al. Parkinson's Disease in Teneurin Transmembrane Protein 4 (TENM4) Mutation Carriers. *Front. Genet.* **2020**, *11*, 598064. [CrossRef]
63. Hor, H.; Francescatto, L.; Bartesaghi, L.; Ortega-Cubero, S.; Kousi, M.; Lorenzo-Betancor, O.; Jiménez-Jiménez, F.J.; Gironell, A.; Clarimón, J.; Drechsel, O.; et al. Missense mutations inTENM4, a regulator of axon guidance and central myelination, cause essential tremor. *Hum. Mol. Genet.* **2015**, *24*, 5677–5686. [CrossRef] [PubMed]
64. Kant, T.; Newe, M.; Winter, L.; Hoffmann, M.; Kämmerer, S.; Klapproth, E.; Künzel, K.; Kühnel, M.; Neubert, L.; El-Armouche, A.; et al. Genetic Deletion of Polo-Like Kinase 2 Induces a Pro-Fibrotic Pulmonary Phenotype. *Cells* **2021**, *10*, 617. [CrossRef] [PubMed]
65. Inglis, K.J.; Chereau, D.; Brigham, E.F.; Chiou, S.-S.; Schöbel, S.; Frigon, N.L.; Yu, M.; Caccavello, R.J.; Nelson, S.; Motter, R.; et al. Polo-like Kinase 2 (PLK2) Phosphorylates α-Synuclein at Serine 129 in Central Nervous System. *J. Biol. Chem.* **2009**, *284*, 2598–2602. [CrossRef] [PubMed]
66. Dong, J.; Hu, Z.; Wu, C.; Guo, H.; Zhou, B.; Lv, J.; Lu, D.; Chen, K.; Shi, Y.; Chu, M.; et al. Association analyses identify multiple new lung cancer susceptibility loci and their interactions with smoking in the Chinese population. *Nat. Genet.* **2012**, *44*, 895–899. [CrossRef]
67. Manning, G.; Whyte, D.B.; Martinez, R.; Hunter, T.; Sudarsanam, S. The Protein Kinase Complement of the Human Genome. *Science* **2002**, *298*, 1912–1934. [CrossRef]
68. Manivannan, J.; Tay, S.; Ling, E.-A.; Dheen, S. Dihydropyrimidinase-like 3 regulates the inflammatory response of activated microglia. *Neuroscience* **2013**, *253*, 40–54. [CrossRef]
69. Kanda, M.; Nomoto, S.; Oya, H.; Shimizu, D.; Takami, H.; Hibino, S.; Hashimoto, R.; Kobayashi, D.; Tanaka, C.; Yamada, S.; et al. Dihydropyrimidinase-like 3 facilitates malignant behavior of gastric cancer. *J. Exp. Clin. Cancer Res.* **2014**, *33*, 66. [CrossRef]
70. Blasco, H.; Bernard-Marissal, N.; Vourc'H, P.; Guettard, Y.O.; Sunyach, C.; Augereau, O.; Khederchah, J.; Mouzat, K.; Antar, C.; Gordon, P.H.; et al. A Rare Motor Neuron Deleterious Missense Mutation in the*DPYSL3*(*CRMP4*) Gene is Associated with ALS. *Hum. Mutat.* **2013**, *34*, 953–960. [CrossRef]
71. Damoulakis, G.; Gambardella, L.; Rossman, K.L.; Lawson, C.; Anderson, K.; Fukui, Y.; Welch, H.C.; Der, C.; Stephens, L.; Hawkins, P.T. P-Rex1 directly activates RhoG to regulate GPCR-driven Rac signalling and actin polarity in neutrophils. *J. Cell Sci.* **2014**, *127*, 2589–2600. [CrossRef]
72. Qin, J.; Xie, Y.; Wang, B.; Hoshino, M.; Wolff, D.W.; Zhao, J.; Scofield, M.A.; Dowd, F.J.; Lin, M.-F.; Tu, Y. Upregulation of PIP3-dependent Rac exchanger 1 (P-Rex1) promotes prostate cancer metastasis. *Oncogene* **2009**, *28*, 1853–1863. [CrossRef] [PubMed]

73. Zhang, D.-Y.; Lei, J.-S.; Sun, W.-L.; Wang, D.-D.; Lu, Z. Follistatin Like 5 (FSTL5) inhibits epithelial to mesenchymal transition in hepatocellular carcinoma. *Chin. Med. J.* **2020**, *133*, 1798–1804. [CrossRef] [PubMed]
74. Vilboux, T.; Lev, A.; Malicdan, M.C.V.; Simon, A.J.; Järvinen, P.; Racek, T.; Puchalka, J.; Sood, R.; Carrington, B.; Bishop, K.; et al. A Congenital Neutrophil Defect Syndrome Associated with Mutations in *VPS45*. *N. Engl. J. Med.* **2013**, *369*, 54–65. [CrossRef] [PubMed]
75. Nayak, S.R.; Harrington, E.; Boone, D.; Hartmaier, R.; Chen, J.; Pathiraja, T.N.; Cooper, K.L.; Fine, J.L.; Sanfilippo, J.; Davidson, N.E.; et al. A Role for Histone H2B Variants in Endocrine-Resistant Breast Cancer. *Horm. Cancer* **2015**, *6*, 214–224. [CrossRef]
76. Shan, Z.; Shakoori, A.; Bodaghi, S.; Goldsmith, P.; Jin, J.; Wiest, J.S. TUSC1, a Putative Tumor Suppressor Gene, Reduces Tumor Cell Growth In Vitro and Tumor Growth In Vivo. *PLoS ONE* **2013**, *8*, e66114. [CrossRef]
77. Zhang, R.; Yu, W.; Liang, G.; Jia, Z.; Chen, Z.; Zhao, L.; Yuan, Y.; Zhou, X.; Li, D.; Shen, S.; et al. Tumor Suppressor Candidate 1 Suppresses Cell Growth and Predicts Better Survival in Glioblastoma. *Cell. Mol. Neurobiol.* **2016**, *37*, 37–42. [CrossRef]
78. Grigorenko, A.P.; Protasova, M.S.; Lisenkova, A.A.; Reshetov, D.A.; Andreeva, T.V.; Garcias, G.D.L.; Roth, M.D.G.M.; Papassotiropoulos, A.; Rogaev, E.I. Neurodevelopmental Syndrome with Intellectual Disability, Speech Impairment, and Quadrupedia Is Associated with Glutamate Receptor Delta 2 Gene Defect. *Cells* **2022**, *11*, 400. [CrossRef]
79. Matsushita, K.; Takeuchi, O.; Standley, D.M.; Kumagai, Y.; Kawagoe, T.; Miyake, T.; Satoh, T.; Kato, H.; Tsujimura, T.; Nakamura, H.; et al. Zc3h12a is an RNase essential for controlling immune responses by regulating mRNA decay. *Nature* **2009**, *458*, 1185–1190. [CrossRef]
80. Tsoi, L.C.; Spain, S.L.; Knight, J.; Ellinghaus, E.; Stuart, P.E.; Capon, F.; Ding, J.; Li, Y.; Tejasvi, T.; Gudjonsson, J.E.; et al. Identification of 15 new psoriasis susceptibility loci highlights the role of innate immunity. *Nat. Genet.* **2012**, *44*, 1341–1348. [CrossRef]
81. Guo, W.; Cai, Y.; Zhang, H.; Yang, Y.; Yang, G.; Wang, X.; Zhao, J.; Lin, J.; Zhu, J.; Li, W.; et al. Association of ARHGAP18 polymorphisms with schizophrenia in the Chinese-Han population. *PLoS ONE* **2017**, *12*, e0175209. [CrossRef]
82. Negredo, P.N.; Edgar, J.R.; Manna, P.T.; Antrobus, R.; Robinson, M.S. The WDR11 complex facilitates the tethering of AP-1-derived vesicles. *Nat. Commun.* **2018**, *9*, 596. [CrossRef]
83. Ouyang, W.-W.; Li, Q.-Y.; Yang, W.-G.; Su, S.-F.; Wu, L.-J.; Yang, Y.; Lu, B. Genetic characteristics of a patient with multiple primary cancers: A case report. *World J. Clin. Cases* **2021**, *9*, 8563–8570. [CrossRef] [PubMed]
84. Abdul-Rahman, P.S.; Lim, B.-K.; Hashim, O.H. Expression of high-abundance proteins in sera of patients with endometrial and cervical cancers: Analysis using 2-DE with silver staining and lectin detection methods. *Electrophoresis* **2007**, *28*, 1989–1996. [CrossRef] [PubMed]
85. Sun, D.; Zhao, Y.Y.; Dai, S.P.; Fang, K.; Dong, L.Y.; Ding, Q. Cloning and analysis of human alpha-1B glycoprotein precursor gene: A novel member of human immunoglobulin superfamily. *Yi Chuan Xue Bao* **2002**, *29*, 299–302. (In Japanese) [PubMed]
86. Kreunin, P.; Zhao, J.; Rosser, C.; Urquidi, V.; Lubman, D.M.; Goodison, S. Bladder Cancer Associated Glycoprotein Signatures Revealed by Urinary Proteomic Profiling. *J. Proteome Res.* **2007**, *6*, 2631–2639. [CrossRef] [PubMed]
87. Tang, J.; Li, Y.; Sang, Y.; Yu, B.; Lv, D.; Zhang, W.; Feng, H. LncRNA PVT1 regulates triple-negative breast cancer through KLF5/beta-catenin signaling. *Oncogene* **2018**, *37*, 4723–4734. [CrossRef]
88. Glasson, S.S.; Askew, R.; Sheppard, B.; Carito, B.; Blanchet, T.; Ma, H.-L.; Flannery, C.R.; Peluso, D.; Kanki, K.; Yang, Z.; et al. Deletion of active ADAMTS5 prevents cartilage degradation in a murine model of osteoarthritis. *Nature* **2005**, *434*, 644–648. [CrossRef] [PubMed]
89. Agajanian, M.J.; Potjewyd, F.M.; Bowman, B.M.; Solomon, S.; LaPak, K.M.; Bhatt, D.P.; Smith, J.L.; Goldfarb, D.; Axtman, A.D.; Major, M.B. Protein proximity networks and functional evaluation of the casein kinase 1 gamma family reveal unique roles for CK1γ3 in WNT signaling. *J. Biol. Chem.* **2022**, *298*, 101986. [CrossRef]
90. Schittek, B.; Sinnberg, T. Biological functions of casein kinase 1 isoforms and putative roles in tumorigenesis. *Mol. Cancer* **2014**, *13*, 231. [CrossRef]
91. Inoue, N.; Watanabe, M.; Yamada, H.; Takemura, K.; Hayashi, F.; Yamakawa, N.; Akahane, M.; Shimizuishi, Y.; Hidaka, Y.; Iwatani, Y. Associations between autoimmune thyroid disease prognosis and functional polymorphisms of susceptibility genes, CTLA4, PTPN22, CD40, FCRL3, and ZFAT, previously revealed in genome-wide association studies. *J. Clin. Immunol.* **2012**, *32*, 1243–1252. [CrossRef]
92. Wallom, K.-L.; Fernández-Suárez, M.E.; Priestman, D.A.; Vruchte, D.T.; Huebecker, M.; Hallett, P.J.; Isacson, O.; Platt, F.M. Glycosphingolipid metabolism and its role in ageing and Parkinson's disease. *Glycoconj. J.* **2021**, *39*, 39–53. [CrossRef] [PubMed]
93. Ryckman, A.E.; Brockhausen, I.; Walia, J.S. Metabolism of Glycosphingolipids and Their Role in the Pathophysiology of Lysosomal Storage Disorders. *Int. J. Mol. Sci.* **2020**, *21*, 6881. [CrossRef]
94. Sardiello, M.; Palmieri, M.; Di Ronza, A.; Medina, D.L.; Valenza, M.; Gennarino, V.A.; Di Malta, C.; Donaudy, F.; Embrione, V.; Polishchuk, R.S.; et al. A Gene Network Regulating Lysosomal Biogenesis and Function. *Science* **2009**, *325*, 473–477. [CrossRef] [PubMed]
95. Olguín, V.; Durán, A.; Heras, M.L.; Rubilar, J.C.; Cubillos, F.A.; Olguín, P.; Klein, A.D. Genetic Background Matters: Population-Based Studies in Model Organisms for Translational Research. *Int. J. Mol. Sci.* **2022**, *23*, 7570. [CrossRef]
96. Rha, A.K.; Maguire, A.S.; Martin, D.R. GM1 Gangliosidosis: Mechanisms and Management. *Appl. Clin. Genet.* **2021**, *14*, 209–233. [CrossRef]

97. Adibekian, A.; Martin, B.; Chang, J.; Hsu, K.-L.; Tsuboi, K.; Bachovchin, D.; Speers, A.; Brown, S.; Spicer, T.; Fernandez-Vega, V.; et al. Characterization of a Selective, Reversible Inhibitor of Lysophospholipase 1 (LYPLA1). In *Probe Reports from the NIH Molecular Libraries Program [Internet]*; National Center for Biotechnology Information (US): Bethesda, MD, USA, 2010.
98. Wu, S.; Cao, R.; Tao, B.; Wu, P.; Peng, C.; Gao, H.; Liang, J.; Yang, W. Pyruvate Facilitates FACT-Mediated γ H2AX Loading to Chromatin and Promotes the Radiation Resistance of Glioblastoma. *Adv. Sci.* **2022**, *9*, 2104055. [CrossRef]
99. Merrill, A.H., Jr. Sphingolipid and Glycosphingolipid Metabolic Pathways in the Era of Sphingolipidomics. *Chem. Rev.* **2011**, *111*, 6387–6422. [CrossRef]
100. Lachmann, R.H.; Vruchte, D.T.; Lloyd-Evans, E.; Reinkensmeier, G.; Sillence, D.; Fernandez-Guillen, L.; Dwek, R.A.; Butters, T.D.; Cox, T.M.; Platt, F.M. Treatment with miglustat reverses the lipid-trafficking defect in Niemann–Pick disease type C. *Neurobiol. Dis.* **2004**, *16*, 654–658. [CrossRef] [PubMed]
101. Elstein, D.; Hollak, C.; Aerts, J.M.F.G.; van Weely, S.; Maas, M.; Cox, T.M.; Lachmann, R.H.; Hrebicek, M.; Platt, F.M.; Butters, T.D.; et al. Sustained therapeutic effects of oral miglustat (Zavesca,*N*-butyldeoxynojirimycin, OGT 918) in type I Gaucher disease. *J. Inherit. Metab. Dis.* **2004**, *27*, 757–766. [CrossRef] [PubMed]
102. Meng, Q.; Hu, X.; Zhao, X.; Kong, X.; Meng, Y.-M.; Chen, Y.; Su, L.; Jiang, X.; Qiu, X.; Huang, C.; et al. A circular network of coregulated sphingolipids dictates lung cancer growth and progression. *Ebiomedicine* **2021**, *66*, 103301. [CrossRef]
103. Pazoki, R.; Vujkovic, M.; Elliott, J.; Evangelou, E.; Gill, D.; Ghanbari, M.; van der Most, P.J.; Pinto, R.C.; Wielscher, M.; Farlik, M.; et al. Genetic analysis in European ancestry individuals identifies 517 loci associated with liver enzymes. *Nat. Commun.* **2021**, *12*, 2579. [CrossRef] [PubMed]
104. Willer, C.J.; Schmidt, E.M.; Sengupta, S.; Peloso, G.M.; Gustafsson, S.; Kanoni, S.; Ganna, A.; Chen, J.; Buchkovich, M.L.; Mora, S.; et al. Discovery and refinement of loci associated with lipid levels. *Nat. Genet.* **2013**, *45*, 1274–1283. [CrossRef] [PubMed]
105. Lee, J.-H.; Yang, D.-S.; Goulbourne, C.N.; Im, E.; Stavrides, P.; Pensalfini, A.; Chan, H.; Bouchet-Marquis, C.; Bleiwas, C.; Berg, M.J.; et al. Faulty autolysosome acidification in Alzheimer's disease mouse models induces autophagic build-up of Aβ in neurons, yielding senile plaques. *Nat. Neurosci.* **2022**, *25*, 688–701. [CrossRef]
106. Stahl-Meyer, J.; Stahl-Meyer, K.; Jäättelä, M. Control of mitosis, inflammation, and cell motility by limited leakage of lysosomes. *Curr. Opin. Cell Biol.* **2021**, *71*, 29–37. [CrossRef] [PubMed]
107. Tan, J.X.; Finkel, T. A phosphoinositide signalling pathway mediates rapid lysosomal repair. *Nature* **2022**, *609*, 815–821. [CrossRef]
108. Alessenko, A.V.; Albi, E. Exploring Sphingolipid Implications in Neurodegeneration. *Front. Neurol.* **2020**, *11*, 437. [CrossRef]
109. Cumin, C.; Huang, Y.-L.; Rossdam, C.; Ruoff, F.; Céspedes, S.P.; Liang, C.-Y.; Lombardo, F.C.; Coelho, R.; Rimmer, N.; Konantz, M.; et al. Glycosphingolipids are mediators of cancer plasticity through independent signaling pathways. *Cell Rep.* **2022**, *40*, 111181. [CrossRef]
110. Snaebjornsson, M.T.; Janaki-Raman, S.; Schulze, A. Greasing the Wheels of the Cancer Machine: The Role of Lipid Metabolism in Cancer. *Cell Metab.* **2019**, *31*, 62–76. [CrossRef]
111. Petersen, N.H.; Olsen, O.D.; Groth-Pedersen, L.; Ellegaard, A.-M.; Bilgin, M.; Redmer, S.; Ostenfeld, M.S.; Ulanet, D.; Dovmark, T.H.; Lønborg, A.; et al. Transformation-Associated Changes in Sphingolipid Metabolism Sensitize Cells to Lysosomal Cell Death Induced by Inhibitors of Acid Sphingomyelinase. *Cancer Cell* **2013**, *24*, 379–393. [CrossRef]
112. Fatehi-Hassanabad, Z.; Chan, C.B. Transcriptional regulation of lipid metabolism by fatty acids: A key determinant of pancreatic β-cell function. *Nutr. Metab.* **2005**, *2*, 1. [CrossRef]
113. Liu, F.; Zhu, X.; Jiang, X.; Li, S.; Lv, Y. Transcriptional control by HNF-1: Emerging evidence showing its role in lipid metabolism and lipid metabolism disorders. *Genes Dis.* **2021**, *9*, 1248–1257. [CrossRef] [PubMed]
114. Pan, G.; Diamanti, K.; Cavalli, M.; Gutiérrez, A.L.; Komorowski, J.; Wadelius, C. Multifaceted regulation of hepatic lipid metabolism by YY1. *Life Sci. Alliance* **2021**, *4*, e202000928. [CrossRef] [PubMed]
115. Magee, N.; Zhang, Y. Role of early growth response 1 in liver metabolism and liver cancer. *Hepatoma Res.* **2017**, *3*, 268–277. [CrossRef] [PubMed]
116. Banerjee, A.; Mahata, B.; Dhir, A.; Mandal, T.K.; Biswas, K. Elevated histone H3 acetylation and loss of the Sp1–HDAC1 complex de-repress the GM2-synthase gene in renal cell carcinoma. *J. Biol. Chem.* **2019**, *294*, 1005–1018. [CrossRef] [PubMed]
117. Martina, J.A.; Diab, H.I.; Lishu, L.; Jeong-A, L.; Patange, S.; Raben, N.; Puertollano, R. The Nutrient-Responsive Transcription Factor TFE3 Promotes Autophagy, Lysosomal Biogenesis, and Clearance of Cellular Debris. *Sci. Signal.* **2014**, *7*, ra9. [CrossRef] [PubMed]
118. Di Malta, C.; Siciliano, D.; Calcagni, A.; Monfregola, J.; Punzi, S.; Pastore, N.; Eastes, A.N.; Davis, O.; De Cegli, R.; Zampelli, A.; et al. Transcriptional activation of RagD GTPase controls mTORC1 and promotes cancer growth. *Science* **2017**, *356*, 1188–1192. [CrossRef]
119. Polager, S.; Ofir, M.; Ginsberg, D. E2F1 regulates autophagy and the transcription of autophagy genes. *Oncogene* **2008**, *27*, 4860–4864. [CrossRef]
120. Seok, S.; Fu, T.; Choi, S.-E.; Li, Y.; Zhu, R.; Kumar, S.; Sun, X.; Yoon, G.; Kang, Y.; Zhong, W.; et al. Transcriptional regulation of autophagy by an FXR–CREB axis. *Nature* **2014**, *516*, 108–111. [CrossRef]
121. Annunziata, I.; van de Vlekkert, D.; Wolf, E.; Finkelstein, D.; Neale, G.; Machado, E.; Mosca, R.; Campos, Y.; Tillman, H.; Roussel, M.F.; et al. MYC competes with MiT/TFE in regulating lysosomal biogenesis and autophagy through an epigenetic rheostat. *Nat. Commun.* **2019**, *10*, 3623. [CrossRef]

122. Song, N.; Song, R.; Ma, P. MiR-340-5p alleviates neuroinflammation and neuronal injury via suppressing STING in subarachnoid hemorrhage. *Brain Behav.* **2022**, *12*, e2687. [CrossRef] [PubMed]
123. Guo, Y.; Gao, Y.; Liu, S. lncRNA XIST is associated with preeclampsia and mediates trophoblast cell invasion via miR-340-5p/KCNJ16 signaling pathway. *Transpl. Immunol.* **2022**, *74*, 101666. [CrossRef]
124. Ou, D.; Wu, Y.; Zhang, J.; Liu, J.; Liu, Z.; Shao, M.; Guo, X.; Cui, S. miR-340-5p affects oral squamous cell carcinoma (OSCC) cells proliferation and invasion by targeting endoplasmic reticulum stress proteins. *Eur. J. Pharmacol.* **2022**, *920*, 174820. [CrossRef] [PubMed]
125. Huang, Z.; Xu, Y.; Wan, M.; Zeng, X.; Wu, J. miR-340: A multifunctional role in human malignant diseases. *Int. J. Biol. Sci.* **2021**, *17*, 236–246. [CrossRef] [PubMed]
126. Liu, Y.; Li, X.; Zhang, Y.; Wang, H.; Rong, X.; Peng, J.; He, L.; Peng, Y. An miR-340-5p-macrophage feedback loop modulates the progression and tumor microenvironment of glioblastoma multiforme. *Oncogene* **2019**, *38*, 7399–7415. [CrossRef] [PubMed]
127. Liu, H.; Li, B.; Qiao, L.; Liu, J.; Ren, D.; Liu, W. miR-340-5p inhibits sheep adipocyte differentiation by targeting *ATF7*. *Anim. Sci. J.* **2020**, *91*, e13462. [CrossRef]
128. Zhu, Y.; Yang, X.; Zhou, J.; Chen, L.; Zuo, P.; Chen, L.; Jiang, L.; Li, T.; Wang, D.; Xu, Y.; et al. miR-340-5p Mediates Cardiomyocyte Oxidative Stress in Diabetes-Induced Cardiac Dysfunction by Targeting Mcl-1. *Oxidative Med. Cell. Longev.* **2022**, *2022*, 3182931. [CrossRef]
129. Priestman, D.A.; Van Der Spoel, A.C.; Butters, T.D.; Dwek, R.A.; Platt, F.M. N-butyldeoxynojirimycin causes weight loss as a result of appetite suppression in lean and obese mice. *Diabetes Obes. Metab.* **2007**, *10*, 159–166. [CrossRef]
130. Chatterjee, S.; Zheng, L.; Ma, S.; Bedja, D.; Bandaru, V.V.R.; Kim, G.; Rangecroft, A.; Iocco, D.; Campbell, S.A. Management of metabolic syndrome and reduction in body weight in type II diabetic mice by inhibiting glycosphingolipid synthesis. *Biochem. Biophys. Res. Commun.* **2020**, *525*, 455–461. [CrossRef]
131. Robinson, D.S. The fluorimetric determination of β-glucosidase: Its occurrence in the tissues of animals, including insects. *Biochem. J.* **1956**, *63*, 39–44. [CrossRef]
132. Shigeto, S.; Katafuchi, T.; Okada, Y.; Nakamura, K.; Endo, F.; Okuyama, T.; Takeuchi, H.; Kroos, M.A.; Verheijen, F.W.; Reuser, A.J.; et al. Improved assay for differential diagnosis between Pompe disease and acid α-glucosidase pseudodeficiency on dried blood spots. *Mol. Genet. Metab.* **2011**, *103*, 12–17. [CrossRef] [PubMed]
133. Beutler, E.; Kuhl, W. Purification and properties of human alpha-galactosidases. *J. Biol. Chem.* **1972**, *247*, 7195–7200. [CrossRef] [PubMed]
134. Mayes, J.S.; Scheerer, J.B.; Sifers, R.N.; Donaldson, M.L. Differential assay for lysosomal alpha-galactosidases in human tissues and its application to Fabry's disease. *Clin. Chim. Acta Int. J. Clin. Chem.* **1981**, *112*, 247–251. [CrossRef]
135. Padeh, B.; Navon, R. Diagnosis of Tay-Sachs disease by hexosaminidase activity in leukocytes and amniotic fluid cells. *Isr. J. Med. Sci.* **1971**, *7*, 259–263.
136. Hauser, E.C.; Kasperzyk, J.L.; D'Azzo, A.; Seyfried, T.N. Inheritance of Lysosomal Acid β-Galactosidase Activity and Gangliosides in Crosses of DBA/2J and Knockout Mice. *Biochem. Genet.* **2004**, *42*, 241–257. [CrossRef] [PubMed]
137. Potier, M.; Mameli, L.; Bélisle, M.; Dallaire, L.; Melançon, S. Fluorometric assay of neuraminidase with a sodium (4-methylumbelliferyl-α-d-N-acetylneuraminate) substrate. *Anal. Biochem.* **1979**, *94*, 287–296. [CrossRef]
138. Seyrantepe, V.; Landry, K.; Trudel, S.; Hassan, J.A.; Morales, C.R.; Pshezhetsky, A.V. Neu4, a Novel Human Lysosomal Lumen Sialidase, Confers Normal Phenotype to Sialidosis and Galactosialidosis Cells. *J. Biol. Chem.* **2004**, *279*, 37021–37029. [CrossRef] [PubMed]
139. Bussink, A.P.; Verhoek, M.; Vreede, J.; der Vlugt, K.G.-V.; Donker-Koopman, W.E.; Sprenger, R.R.; Hollak, C.E.; Aerts, J.M.F.G.; Boot, R.G. Common G102S polymorphism in chitotriosidase differentially affects activity towards 4-methylumbelliferyl substrates. *FEBS J.* **2009**, *276*, 5678–5688. [CrossRef]
140. Schoonhoven, A.; Rudensky, B.; Elstein, D.; Zimran, A.; Hollak, C.E.; Groener, J.E.; Aerts, J.M. Monitoring of Gaucher patients with a novel chitotriosidase assay. *Clin. Chim. Acta* **2007**, *381*, 136–139. [CrossRef]
141. Lau, K.H.; Onishi, T.; Wergedal, J.E.; Singer, F.R.; Baylink, D.J. Characterization and assay of tartrate-resistant acid phosphatase activity in serum: Potential use to assess bone resorption. *Clin. Chem.* **1987**, *33*, 458–462. [CrossRef]
142. Goodlad, G.A.J.; Mills, G.T. The acid phosphatases of rat liver. *Biochem. J.* **1957**, *66*, 346–354. [CrossRef]
143. di Matteo, G.; Orfeo, M.A.; Romeo, G. Human α-fucosidase: Purification and properties. *Biochim. Biophys. Acta (BBA)-Enzym.* **1976**, *429*, 527–537. [CrossRef]
144. Li, C.; Qian, J.; Lin, J.-S. Purification and characterization of α-L-fucosidase from human primary hepatocarcinoma tissue. *World J. Gastroenterol.* **2006**, *12*, 3770–3775. [CrossRef] [PubMed]
145. Neville, D.C.; Coquard, V.; Priestman, D.A.; te Vruchte, D.J.M.; Sillence, D.J.; Dwek, R.A.; Platt, F.M.; Butters, T.D. Analysis of fluorescently labeled glycosphingolipid-derived oligosaccharides following ceramide glycanase digestion and anthranilic acid labeling. *Anal. Biochem.* **2004**, *331*, 275–282. [CrossRef] [PubMed]
146. R Core Team. *A Language and Environment for Statistical Computing*; R Foundation for Statistical Computing: Vienna, Austria, 2020.

147. Kirby, A.; Kang, H.M.; Wade, C.M.; Cotsapas, C.; Kostem, E.; Han, B.; Furlotte, N.; Kang, E.Y.; Rivas, M.; Bogue, M.A.; et al. Fine Mapping in 94 Inbred Mouse Strains Using a High-Density Haplotype Resource. *Genetics* **2010**, *185*, 1081–1095. [CrossRef]
148. Rebhan, M. GeneCards: Integrating information about genes, proteins and diseases. *Trends Genet.* **1997**, *13*, 163. [CrossRef]